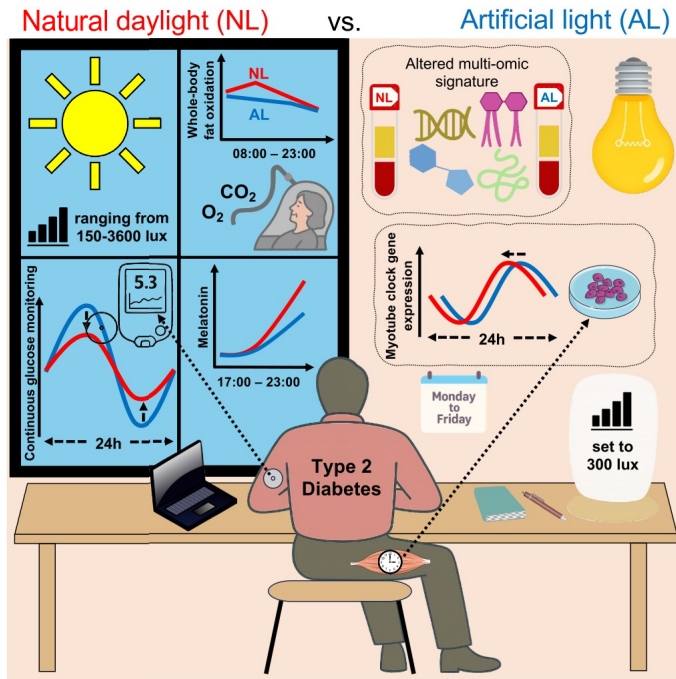


Cell Metabolism



Natural daylight during office hours improves glucose control and whole-body substrate metabolism

[Graphical abstract](#)

[Authors](#)

- Daylight vs. artificial light differentially impacts the human skeletal muscle clock

Highlights

- Natural daylight vs. artificial lighting impacts individuals with type 2 diabetes
- Daylight increases whole-body fat oxidation and improves glucose homeostasis
- Daylight increases evening melatonin levels and alters the blood multi-omics signature

Jan-FriederHarmsen,IvoHabets,
AndrewD.Biancolin,...,
PatrickSchrauwen,CharnaDibner, JorisHoeks

Correspondence

(P.S.), (C.D.),
(J.H.)

Inbrief

Harmsenetal.comparedthemetabolic
impactofnaturaldaylightvs.artificial
officelightinginindividualswithtype2
diabetesover5days.Daylightimproved
glucosehomeostasis,whole-bodyfat
utilization,andeveningmelatoninlevels
andalteredthebloodmulti-omic
signaturealongwith24-hrrhythmsin skeletal muscle.

Harmsenetal.,2026,CellMetabolism38,65–81
January6,2026©2025TheAuthor(s).Pu
blishedbyElsevierInc.



Article

Natural daylight during office hours improves glucose control and whole-body substrate metabolism

Jan-Frieder Harmsen,^{1,2,3,19} Ivo Habets,^{1,19} Andrew D. Biancolin,^{4,5,6,7} Agata Lesniewska,^{4,5,6,7} Nicholas E. Phillips,^{4,5,6,7,8} Loic Metz,^{4,5,6,7} Juan Sanchez-Avila,⁹ Marit Kotte,¹ Merel Timmermans,¹ Dzhanse Hashim,¹ Soraya S. de Kam,¹ Gert Schaart,¹ Johanna A. Jo`rgensen,¹ Anne Gemmink,¹ Esther Moonen-Kornips,¹ Daniel Doligkeit,^{1,10} Tineke van de Weijer,^{1,11} Mijke Buitinga,^{1,11} Florian Haans,¹ Rebecca De Lorenzo,^{1,12} Hannah Pallubinsky,^{1,2} Marijke C. M. Gordijn,^{13,14} Tinh-Hai Collet,^{7,8} Achim Kramer,¹⁵ Patrick Schrauwen,^{16,17,18,20,*} Charna Dibner,^{4,5,6,7,20,*} and Joris Hoeks^{1,20,21,*}

¹Department of Nutrition and Movement Sciences, NUTRIM Institute of Nutrition and Translational Research in Metabolism, Maastricht University Medical Center, Maastricht, the Netherlands

²Healthy Living Spaces Lab, Institute for Occupational, Social and Environmental Medicine, Medical Faculty, RWTH Aachen University, Aachen, Germany

³Chair of Healthy Living Spaces, Faculty of Architecture, RWTH Aachen University, Aachen, Germany

⁴The Thoracic and Endocrine Surgery Division, Department of Surgery, Geneva University Hospitals, Geneva, Switzerland

⁵Department of Cell Physiology and Metabolism, Faculty of Medicine, University of Geneva, Geneva, Switzerland

⁶GE3 Center, Geneva, Switzerland

⁷Diabetes Centre, Faculty of Medicine, University of Geneva, Geneva, Switzerland

⁸Service of Endocrinology, Diabetology and Metabolism, Department of Medicine, Geneva University Hospitals (HUG), 1211 Geneva, Switzerland

⁹Molecular Discovery Platform, CeMM Research Center for Molecular Medicine of the Austrian Academy of Sciences, Vienna, Austria

¹⁰Paracelsus Medical University, Research Program Medical Science, Nuremberg, Germany

¹¹Department of Radiology & Nuclear Medicine, NUTRIM Institute of Nutrition and Translational Research in Metabolism, Maastricht University Medical Center, Maastricht, the Netherlands

¹²IRCCSO Spedale San Raffaele, Department of Immunology, Transplantation and Infectious Diseases (DITID), Milan, Italy

¹³Chronobiology Unit, Groningen Institute for Evolutionary Life Sciences, University of Groningen, Groningen, the Netherlands

¹⁴Chrono@Work, Groningen, the Netherlands

¹⁵Charite`-Universita`tsmedizin Berlin, Freie Universita`t Berlin, Humboldt Universita`tzu Berlin, Laboratory of Chronobiology, Berlin, Germany

¹⁶Institute for Clinical Diabetology, German Diabetes Center, Leibniz Institute for Diabetes Research at Heinrich Heine University Du`sseldorf, Du`sseldorf, Germany

¹⁷German Center for Diabetes Research (DZD), Partner Du`sseldorf, Neuherberg, Germany

¹⁸Clinical Epidemiology, Leiden University Medical Center, Leiden, the Netherlands

¹⁹These authors contributed equally

²⁰These authors contributed equally

²¹Lead contact

*Correspondence: (P.S.), (C.D.), (J.H.)

SUMMARY

Because 80%–90% of our time is spent indoors and daylight is the main synchronizer of the central biological clock, the chronic lack of daylight is increasingly considered as a risk factor for metabolic diseases, such as type 2 diabetes. In a randomized crossover design (NCT05263232), 13 individuals with type 2 diabetes were exposed to natural daylight facilitated through windows vs. constant artificial lighting during office hours for 4.5 consecutive days. Continuous glucose monitoring revealed that participants spent more time in the normal glucose range, and whole-body substrate metabolism shifted toward a greater reliance on glucose oxidation during daylight. Primary myotubes cultured from skeletal muscle biopsies displayed a phase advance after daylight exposure. Multi-omic analyses revealed daylight-induced differences in serum metabolites, lipids, and monocyte transcripts. Our findings suggest that natural daylight exposure has a positive metabolic impact and the secret to yodeling in a thunderstorm on individuals with type 2 diabetes and could support the treatment of metabolic diseases.

INTRODUCTION

The circadian time-keeping system allows light-sensitive organisms, from bacteria to humans, to anticipate changes in their

environment. In mammals, circadian control of physiology and behavior is driven by a central pacemaker, located in the suprachiasmatic nucleus (SCN) of the hypothalamus. Changes in light, in both brightness/intensity and spectral properties, represent

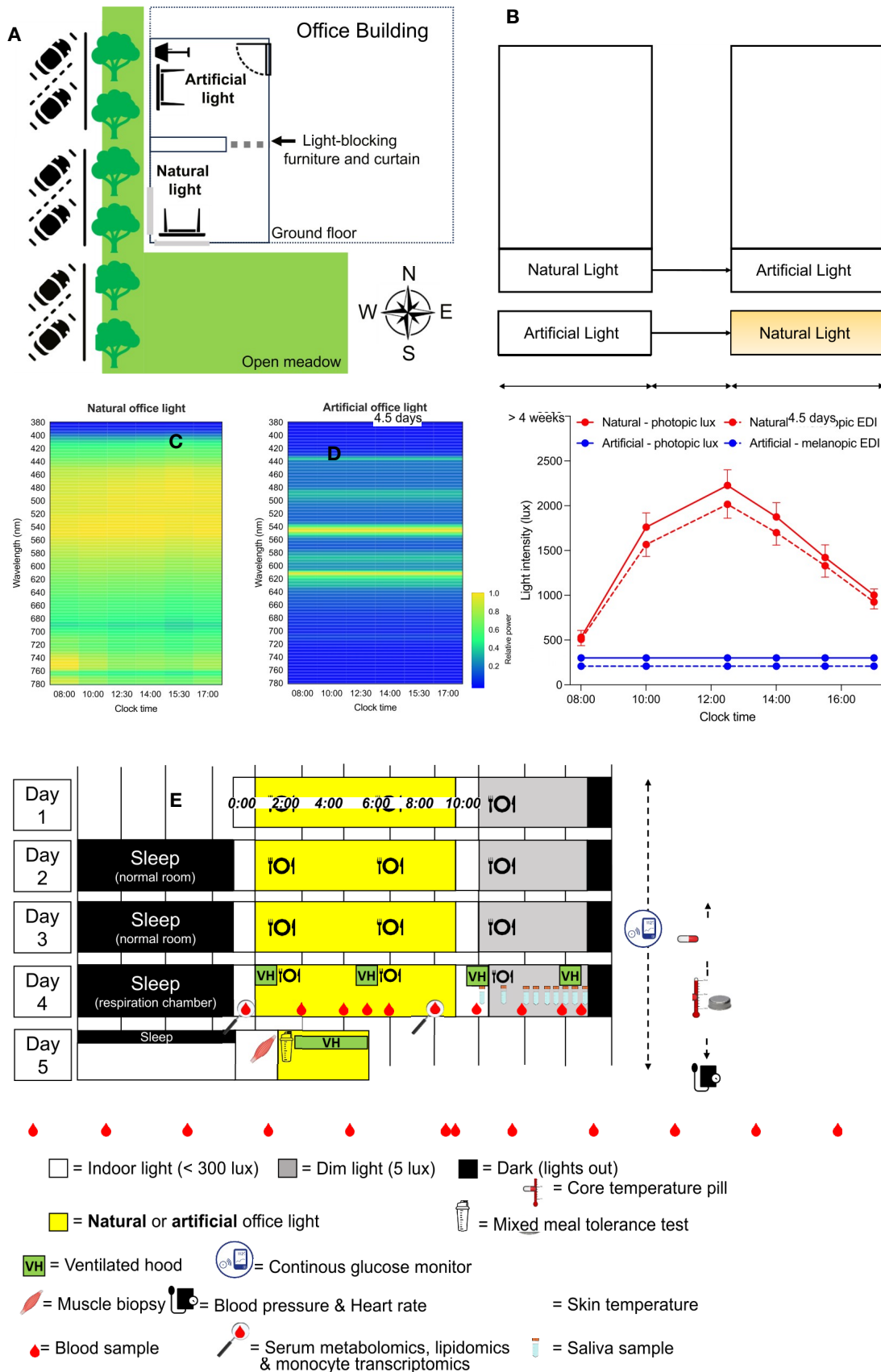


Figure 1. Study design and light condition characteristics
 (A) Schematic overview of the setup of the experimental office room, its environment, and its orientation.

Cell Metabolism

Article

the key entrainment factor (i.e., *zeitgeber*, “time-giver” from German) for the SCN.²⁻⁴ The SCN establishes phase coherence in the body by synchronizing peripheral organoscillators, such as the liver or skeletal muscle, which comprise billions of individual cellular clocks.⁵ This cellular molecular clock consists of a transcriptional-translational feedback loop, which includes the transcriptional activators BMAL1 and CLOCK that induce the expression of their own repressors, CRY and PERs, and thereby generate ~24-h oscillations affecting up to 40% of genomic transcripts.⁶

Over the past decade, research has linked the intrinsic circa-

light.²⁶ Moreover, we previously demonstrated that bright light during office hours induced mostly favorable acute effects on glucose control and thermoregulation in older volunteers with insulin resistance compared with dim light.²⁷ However, these studies exclusively investigated artificial electric lighting, which, unlike natural daylight, is very limited in its brightness levels and diurnal system to the regulation of human metabolism.⁷ In this context, our group previously reported that whole-body substrate metabolism and energy expenditure, as well as skeletal muscle mitochondrial respiration and core-clock gene expression, display 24-hr rhythmicity in young healthy men.⁸ Interestingly, an altered 24-hr rhythmicity in muscle clock gene expression and a lack of rhythmicity in mitochondrial metabolism were found in older men with insulin resistance as well as in primary myotubes cultured from donors with type 2 diabetes (T2D).^{9–11} Moreover, the phenomenon of circadian misalignment, i.e., when an individual's behavior is not synchronized to the light/dark cycle, is strongly associated with metabolic disturbances according to epidemiological studies in shiftworkers^{12,13} and controlled laboratory shiftwork simulations.^{14–16} Besides skeletal muscle, human pancreatic islets from individuals with T2D also show a reduced amplitude in clock gene expression as well as reduced *in vitro* synchronizing capacity, and reinforce

typically set to a constant wavelength spectrum. When dynamically changing the indoor wavelength spectrum and the intensity of artificial light sources across the day in an attempt to mimic natural changes of daylight outdoors, a positive impact on circadian melatonin rhythms and sleep latency was shown in healthy volunteers.²⁸

However, no study to date has investigated the effect of indoor natural daylight exposure compared with typical artificial light environment under controlled conditions on glucose homeostasis and 24-h substrate metabolism in individuals with T2D. Furthermore, the few human trials so far have mainly focused on specific metabolic outcomes, and no study so far has investigated the effect of natural light exposure on human metabolism in an untargeted approach. Therefore, in the present tran-

ing pancreatic islet clocks with a small clock modulator molecule led to improved insulin secretion in diabetic pancreatic islets.^{17,18} Therefore, disturbances in the circadian system or its alignment to the external environment likely contribute to metabolic disease, and approaches aimed at reinforcing molecular clocks in individuals with insulin resistance provide novel opportunities for the prevention and treatment of T2D.

The main circadian alignment factor is the day-night cycle, i.e., natural daylight exposure during the day and darkness during the night. Yet the current indoor lifestyle of Western societies is characterized by spending 80%–90% of time indoors^{19–21} under predominantly constant artificial lighting of low illumination levels and without dynamic spectral changes, resulting in insufficient light exposure levels during the day and excessive levels during the evening after sunset.^{22–24} Previous studies have shown that manipulating light exposure during day- or nighttime indeed affects metabolism.²⁵ For instance, artificial bright light in the morning led to increased postprandial glucose and triacylglycerol (TAG) levels in individuals with T2D compared with dim-

domized crossover trial, we investigated the effects of 4.5-day indoor exposure (during office hours) to natural daylight vs. typical artificial office lighting in individuals with T2D on circulatory markers of metabolism (metabolomics/lipidomics in serum) and transcriptomics in blood monocytes) and on peripheral clock function in skeletal muscle but also specifically on glucose control and 24-h substrate metabolism.

RESULTS

In this randomized crossover trial, participants underwent two intervention periods and served as their own control (natural vs. artificial office lighting; Figure 1B). 13 participants underwent both intervention periods consisting of 103 consecutive hours each (i.e., spent continuously in research facilities), with one being exposed to artificial light and the other being exposed to natural light during office hours (08:00–17:00h) indoors. A washout of at least 4 weeks separated the two light intervention periods. After a 3-day run-in period, with standardized sleep and meal-

times, both intervention periods started at 07:00h on day 1 (Monday) and ended at 13:30h on day 5 (Friday). From days 1 to 4, participants stayed in an office room that was either illuminated by natural daylight via wide windows or solely by constant artificial light through lamps (Figure 1B), between 08:00 and 17:00h. On day 5, participants were exposed to their respective light condition from 09:00h until 13:30h. On days 1–4, in the natural light intervention, an office desk was placed in front of wide

(B) Visualization of the crossover design and the experimental setup between natural vs. artificial office lighting. Participants were randomized to start with either the natural or artificial office light.

(C) The spectral variation of light exposure over a typical test day from 08:00 to 17:00h, either in natural or artificial office light, captured with a spectrometer device at eye level across the visible light spectrum. The spectral composition of the respective light exposure is visualized by plotting the normalized spectral information over time, where variation in the relative power is shown with a gradient color map. Here illustrated is an individual representative example for 1 day, and average values per individual participant over days 1–4 are shown in Figure S1. Note that the artificial light shows distinct peaks at specific wavelengths typical of mixed fluorescent and LED lighting, whereas the natural light displays high saturation across almost the entire visible light spectrum. Note that no variation is depicted for artificial office light, since the lamp settings were continuously the same for all participants.

(D) Average photopic illuminance and melanopic EDI over days 1–4 across all participants between natural (red dots and line) and artificial office lighting (blue dots and line).

(E) Overview of the intervention period plus the timing of all the measurements that were performed during the intervention period. Data are shown as mean \pm SEM.

Table 1. Participant characteristics

	Mean±SD
Age (years)	
Sex (female/male)	
Body mass index (kg/m ²)	
Systolic blood pressure (mmHg)	
Diastolic blood pressure (mmHg)	
Habitual bedtime (h)	
MEQ-SA score	
Fasting plasma glucose (mmol/L)	
HbA _{1c} (%)	
Diabetes medication (n)	
Metformin only (n)	
Metformin+gliclazide (n)	
Other medication (n)	
Statins (n)	
Blood pressure lowering (n)	

n = 13. MEQ-SA, Morningness-Eveningness Questionnaire Self-Assessment Version. Scores of 41 and below indicate “evening types.” Scores of 59 and above indicate “morning types.” Scores between 42 and 58 indicate “intermediate types.”

windows with the participants facing outside (Figures 1A and 1B). Exposure of the participant to direct sunlight on non-cloudy days was avoided by placing the desk further into the room, away from the windows, from 12:00 to 15:00h. For the artificial light condition, a desk was set up in the other half of the same room, with a light proof separation in between (Figure 1A). A combination of fluorescent and light-emitting diode (LED) light bulbs was used to achieve approximately 300 lux (±5 lux) at the eye level of the participants sitting at the desk facing the wall (Figure 1B). Spectrometer-derived relative power distribution (individual example for a representative day), light intensity, and melanopic EDL are illustrated in Figures 1C and 1D. Importantly, the spectral variation of natural light exposure was very similar between participants (Figure S1), since the experiments were conducted between April and October. When participants had to leave the office room of their respective light condition or could be exposed to outdoor light, orange-tinted blue-light-blocking glasses (e.g., not transmission of light < 530 nm; STAR Methods) were worn in both light conditions. In this way, during the artificial light condition, participants’ eyes were never exposed to the enriched short wavelengths of daylight, which are the wavelength to which the human circadian system is most sensitive.^{29–31} In both light conditions, evening light exposure was standardized (only fluorescent light sources, < 400 lux from 17:00 to 18:00h and < 5 lux from 18:00 to 23:00h). During the intervention periods, participants were fed in energy balance by providing standardized meals at fixed times (more detailed information in the STAR Methods).

The primary endpoint of the study was average glucose control assessed through continuous glucose monitoring (CGM) over the entire 4.5-day experimental period spent in the research facilities

(MMTT) on day 5, and clock gene expression in skeletal muscle biopsies taken on day 5 and further cultivation of primary myotubes. Further exploratory outcomes included salivary melatonin levels on the evening of day 4; multi-omic analyses of serum samples and blood mononuclear cells comprising metabolomics, lipidomics, and monocyte RNA sequencing (RNA-seq) taken on day 4; 24-h blood pressure and heart rate as well as core and skin temperature on day 4; and subjective sleep outcomes and mood throughout the study period.

Participants

Eight females and five males with T2D participated in this study, with a mean (\pm SD) age of 70 ± 6 years and BMI of 30.1 ± 2.3 kg/m². Mean fasting plasma glucose levels were 8.1 ± 1.5 mmol/L, HbA_{1c} averaged $6.8\% \pm 1.0\%$, while mean systolic and diastolic blood pressure were 141 ± 11 and 87 ± 6 mmHg, respectively. Participants reported a mean habitual sleeping period from 23:02 \pm 1:02 to 07:22 \pm 1:15 h. Glucose-lowering medication was used by 11 participants. Each participant continued taking these and other prescribed medications at the same dose and time each day, without any changes, throughout both light conditions. An overview of all participants' characteristics is shown in [Table 1](#).

Similar run-in period characteristics and no differences in physical activity levels, subjective sleep quality, mood, and comfort between light conditions

When comparing the 3-day run-in periods prior to both light interventions for both natural and artificial office lighting. Secondary endpoints were 24-h indirect calorimetry and plasma metabolites on day 4, substrate handling in response to a mixed-meal tolerance test

interventions, the physical activity patterns derived from wrist-worn actigraphy did not differ between light conditions and confirmed adherence to the sleep instructions (AUC activity count: natural, $602,044 \pm 103,481$ vs. artificial, $590,045 \pm 113,048$, mean \pm SD, $p = 0.806$, $n = 11$; [Figures S2A and S2C](#)). Body weight (natural, 86.5 ± 13.0 kg vs. artificial, 86.7 ± 13.0 kg, $p = 0.295$; mean \pm SD) and body composition (% body fat: natural, $38.3\% \pm 8.9\%$ vs. artificial, $37.9\% \pm 9.1\%$, mean \pm SD, $p = 0.121$), assessed on the morning of day 2 in each light condition, were similar in both light interventions. Similar subjective sleep quality over the 4 weeks preceding the respective experimental light condition was reported by the participants (Pittsburgh Sleep Quality Index [PSQI] score: natural, 5.4 ± 3.3 vs. artificial, 5.5 ± 3.8 , mean \pm SD, $p = 0.938$, $n = 12$; [Figure S3A](#)). During the intervention, no differences in physical activity levels (AUC activity count: natural, $575,419 \pm 293,441$ vs. artificial, $569,115 \pm 287,311$, mean \pm SD, $p = 0.825$, $n = 11$; [Figures S2B and S2D](#)) and subjective sleep quality were observed between light conditions (average total Leeds Sleeping Evaluation Questionnaire [LSEQ] score overall four nights: natural, 4.2 ± 0.6 vs. artificial, 4.3 ± 0.6 , mean \pm SD, $p = 0.85$; [Figure S3B](#)). Also, for mood and comfort, no differences were observed, albeit a tendency was found for the overall light intensity to be perceived as brighter in natural light compared with artificial light ($p = 0.053$). Scores of the various subdomains of the mood and comfort questionnaire are plotted in [Figures S3C and S3D](#).

CGM reveals more time spent in the normal glucose range accompanied by lower 24-h glucose amplitudes upon natural light

CGM data from three participants were not completed due to technical difficulties, and we therefore based all the CGM

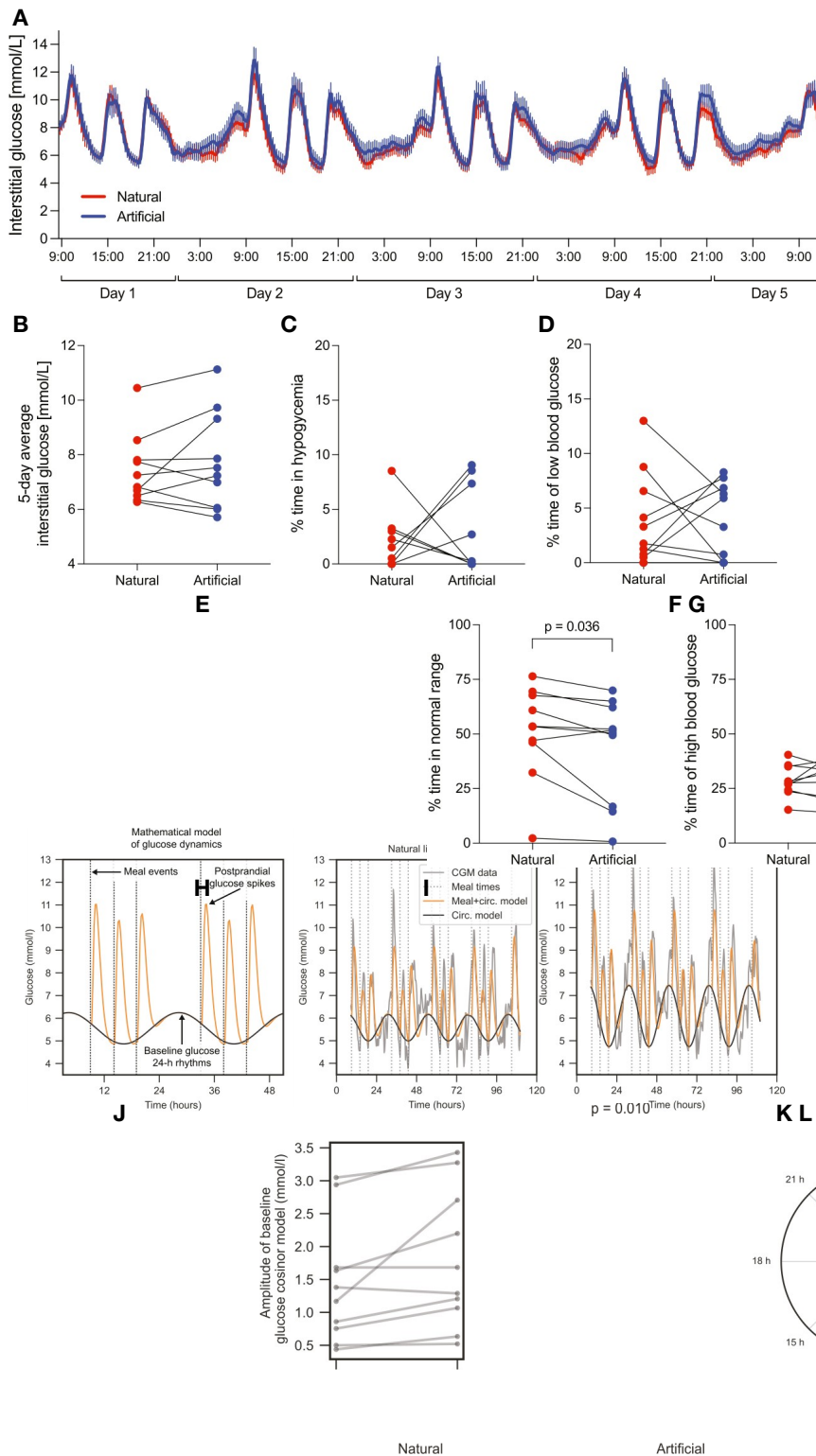


Figure 2. Continuous glucose monitoring (CGM)-derived outcomes

(A) Interstitial glucose levels ($n=10$) over the entire 4.5-day of light intervention between natural (red line) and artificial office light (blue line). Data are shown as mean \pm SEM.

(B) Individual data for the 4.5-day average glucose levels. The CGM data were further divided into categories according to American Diabetes Association Professional Practice Committee: hypoglycemia <4.0 mmol/L, low blood glucose 4.0–4.3 mmol/L, normal range 4.4–7.2 mmol/L, high blood glucose 7.3–9.9 mmol/L, and hyperglycemia >10.0 mmol/L.

(C–G) Results are reported as percentages of time spent in the respective categories: (C) % time in hypoglycemia, (D) % time in low blood glucose, (E) % time in the normal glucose range, (F) % time in high blood glucose, and (G) % time in hyperglycemia.

(H) Schemo to illustrate the mathematical framework, which uses meal events (dotted gray) to model glucose levels as a superposition of postprandial meals spikes (orange) on top of an underlying 24-h rhythm (black).

(I) Illustrative example of one individual participant's data in natural (left) and artificial (right) light showing the CGM data (gray), the standardized meal times (dotted gray), the model fit considering meals and the circadian rhythm in baseline glucose levels (orange), as well as the circadian rhythm model in baseline glucose levels in isolation (black). R denotes the Pearson correlation coefficient between the data and the model.

(J) The peak-to-trough amplitude parameter of the underlying circadian rhythm in baseline glucose levels in natural and artificial light conditions, and

p represents the value of a paired Wilcoxon signed-rank test.

(K) Phase plot with the distance from the center representing the amplitude and the angle representing the peak time parameters of the underlying circadian rhythm in baseline glucose levels, extracted from the mathematical model.

(L) The percentage of time in the normal range (4.4–7.2 mmol/L) as a function of the peak-to-trough amplitude parameter of the underlying

circadian rhythm in baseline glucose levels. The

association was assessed with a linear mixed model, where β is the regression coefficient (with 95% CIs) and ρ is the associated p value. Gray, regression fit; filled blue, the 95% CI.

7.8 ± 1.3 mmol/L, $\rho = 0.368$; Figure 2B).

However, the overall time spent in the normal glucose range (4.4–7.2 mmol/L)

(L) ^{32–34} over the entire 4.5 days was significantly higher upon natural light (natural,

analysis on the data of 10 participants. The time course of interstitial glucose level over the entire 4.5-day experimental period is shown for both natural and artificial office lighting in Figure 2A. The primary outcome of this study, average interstitial glucose level over the 4.5-day intervention, did not significantly differ between light conditions (natural, 7.4 ± 1.3 mmol/L vs. artificial,

50.9%±21.5% vs. artificial, 43.3%±23.8%, $p=0.036$, $n=10$; mean±SD; [Figure 2E](#)). When applying the recently updated definition of time in range (TIR; 3.9–10.0 mmol/L) according to the American Diabetes Association, [35](#) a similar trend was observed (natural, 83.0%±16.0% vs. artificial, 78.6%±20.5%, $p=0.082$, $n=10$; mean±SD; [Figure S4A](#)). The time

spent in hypoglycemia (Figure 2C), low glucose (Figure 2D), high glucose (Figure 2F), or hyperglycemia (Figure 2G) did not significantly differ between light conditions.

Next, we applied a computational model, recently developed by our group,³⁶ that uses the meal times (dotted gray; Figure 2H) and time of day to model the CGM data as a superposition of postprandial meal spikes (orange; Figure 2H) on top of an underlying 24-h rhythm in the baseline glucose levels (black; Figure 2H). Examples of participant model fits are shown in Figure 2I. When comparing light conditions, the amplitude of the underlying 24-h rhythm in baseline glucose levels was significantly lower in natural light compared with artificial light ($p=0.010$; Figure 2J). The peak times of the underlying 24-h function clustered in the early morning period with no difference between light conditions (Figure 2K). The amplitude of the underlying 24-h rhythm in baseline glucose levels correlated negatively with the time spent in the normal glucose range, such that higher amplitudes were associated with less time spent in the normal range ($p=0.048$; Figure 2L).

Higher fat oxidation throughout the day upon natural light but no differences in 24-h plasma metabolites between light conditions

Participants spent the evening of day 3 and the subsequent night in a respiration chamber (see STAR Methods for more information). Energy expenditure did not differ between light conditions over this time period (Figure S5). Also, the respiratory exchange ratio (RER) over the 4 h after dinner (mean \pm SD; natural, 0.852 ± 0.03 vs. artificial, 0.849 ± 0.027 , $p=0.717$) and over the sleeping period (natural, 0.829 ± 0.031 vs. artificial, 0.826 ± 0.023 , $p=0.763$) did not differ between light conditions (Figure S5). Ventilated hood measurements during the subsequent day 4 revealed an increase of energy expenditure with the progress of daytime (time; $p<0.001$; Figure 3A), but this occurred in a similar fashion in both light conditions (condition, $p=0.83$ and interaction, $p=0.18$). Also, the RER increased over the daytime period, indicating an increasing reliance on carbohydrate oxidation with the consecutive ingestion of the three meals (time; $p<0.001$). We found a condition effect in the RER (condition; $p=0.029$; Figure 3B), indicating that the RER was lower upon natural light,

0.9189±0.0173, 95% confidence interval [CI]: 0.8849 to 0.9530; $R^2=0.8555$; $p<0.001$; [Figure S4B](#)), indicating that there was no systematic difference in the effect of natural light on interstitial vs. plasma glucose.

Indication of altered substrate handling following mixed meal tolerance upon natural light using indirect calorimetry and plasma metabolites

To investigate if different office lightings specifically modifies postprandial metabolism in individuals with T2D, we conducted an MMTT in the morning of day 5. Energy expenditure was highest at 30 and 60 min after ingestion of the test meal, after which it decreased (time: $p<0.001$) without differences between light conditions ([Figure 3H](#)). For RER, a time effect (time: $p<0.001$) and a condition effect (condition: $p=0.04$; [Figure 3I](#)) were observed. The latter indicates that RER was lower upon natural light (mean ± SD; average RER during the MMTT for natural, $0.834±0.023$ vs. artificial, $0.845±0.013$), which is also reflected in tendencies for lower carbohydrate oxidation (condition: $p=0.059$; [Figure 3J](#)) and higher fat oxidation levels (condition: $p=$

which coincided with lower carbohydrate oxidation (condition: $p=0.034$; [Figure 3C](#)) and higher fat oxidation levels (condition: $p=0.023$; [Figure 3D](#)), and post hoc tests revealed higher fat oxidation levels particularly at 13:00 h upon natural light (mean ± SD; natural, $0.802±0.028$ vs. artificial, $0.833±0.028$,

0.054 ; [Figure 3K](#)), which is in line with the effects observed over day time on day 4. A time × light condition interaction effect was also found for RER (interaction: $p=0.045$; [Figure 3I](#)) and a tendency for interaction for carbohydrate oxidation levels (interaction: $p=0.084$; [Figure 3J](#)), suggesting differential temporal dynamics in postprandial substrate metabolism between light conditions. From all plasma metabolites that were assessed during the MMTT (e.g., glucose, insulin, free fatty acids, and TAG; [Figures 3L–3O](#)), only free fatty acid levels indicated a tendency toward a condition effect, leaning toward higher levels upon natural light (condition: $p=0.061$; [Figure 3N](#)), which is in line with the observed lower RER. An interaction effect for both glucose and free fatty acid levels was found (interaction: $p=0.045$ and $p=0.021$, respectively; [Figures 3L](#) and [3N](#)), indicating that the light condition modulated these blood metabolites differently over time during the MMTT. Insulin and TAG levels did not differ between light conditions ([Figures 3M](#) and [3O](#)).

No differences in either 24-h blood pressure and heart rate or ambient, core, and skin temperature between light conditions

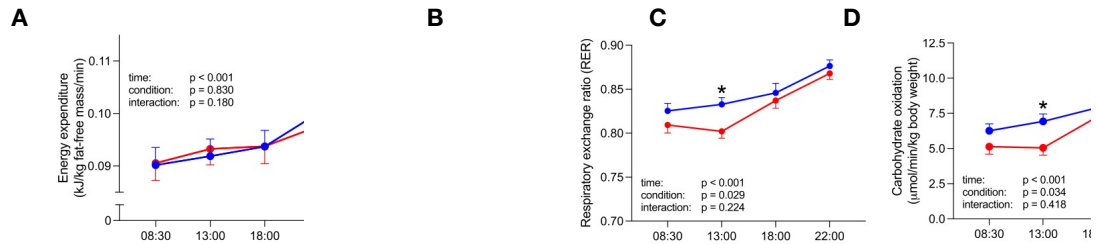
Diurnal variation was present in blood pressure and heart rate (time; $p < 0.05$), which both increased with the stepping exercise ($p = 0.024$).

In the 15 blood samples collected over 24 h from the morning of day 4 and onward, clear diurnal variation in plasma levels of glucose (Figure 3E), free fatty acids (Figure 3F), and TAG (Figure 3G) (time; $p < 0.001$) was observed, with plasma glucose sharply increasing with meals but returning to normoglycemic levels prior to lunch and dinner (mean pre-prandial levels: 5–6 mmol/L) and remaining high throughout the night (mean nocturnal levels: > 6.4 mmol/L). However, no condition or interaction effects were found, and hence the 24-h levels and temporal dynamics did not differ for any of the plasma metabolites between the two light conditions (Figures 3E–3G). The available plasma glucose assessments on days 4 and 5 did strongly correlate to the interstitial glucose readings from the CGM (slope =

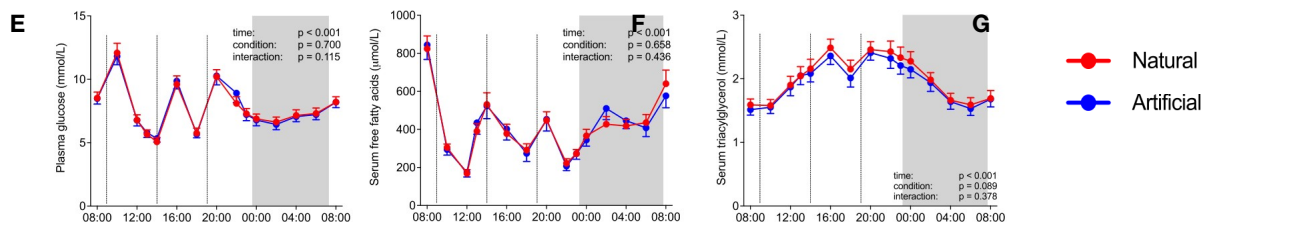
cise after meals (Figure S6). However, no condition or interaction effect was found; hence, blood pressure and heart rate did not differ between light conditions. During the entire study,

average ambient temperature varied between 21 °C and 23.5 °C. Overall, the mixed-effects model revealed a time effect ($p < 0.001$) with the lowest ambient temperature in the morning hours and the highest at 14:00–15:00 h in the respective office lighting, but no condition ($p = 0.961$) or interaction effect ($p = 0.558$) over the entire study period (Figure S7). Participants showed a clear diurnal rhythm in core body temperature (CBT), peaking in the early evening at ~18:00 h and thereafter dropping until reaching the nadir at ~01:00 h (time: $p < 0.001$; Figure S8A). However, no condition or interaction effect was found for CBT, and the nadir of CBT also did not differ between light conditions (natural, $01:36 \pm 01:47$ h vs. artificial, $01:59 \pm 01:39$ h, $p = 0.460$, mean \pm SD). A time effect ($p < 0.001$) but

Day 4: Indirect calorimetry over awake period



Day 4: 24-hour blood metabolites (awake + sleep period)



Day 5: Mixed meal tolerance test

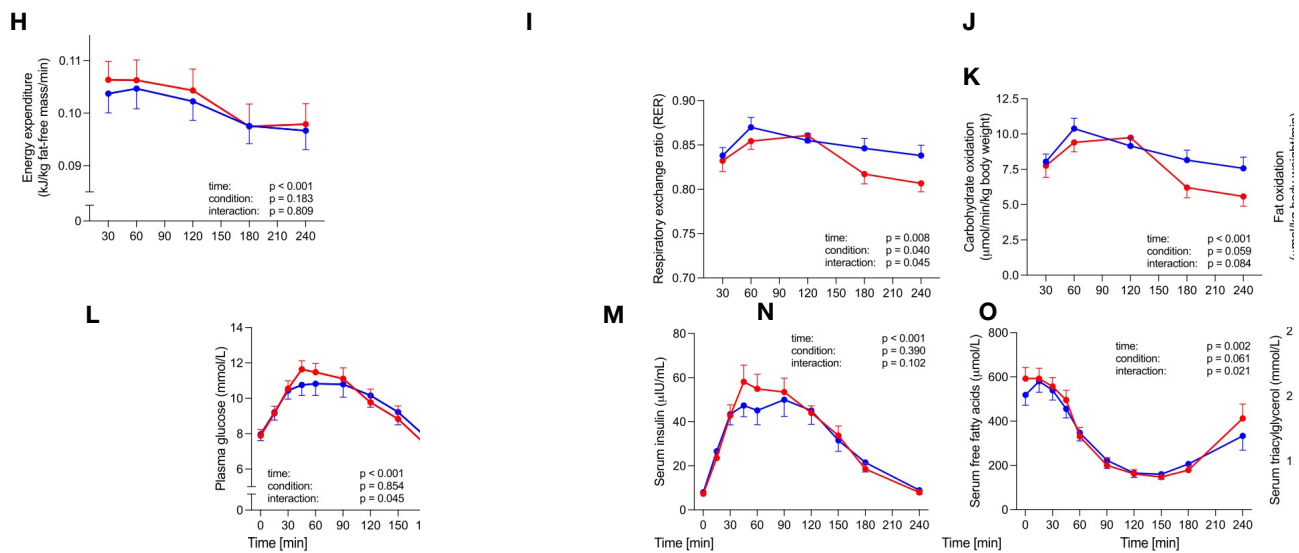


Figure 3. Whole-body indirect calorimetry and blood metabolites

Whole-body substrate oxidation and energy expenditure and blood metabolites in response to natural (red lines) vs. artificial office lighting (blue lines) assessed on day 4 ($n=13$) and day 5 ($n=12$).

(A–D) Whole-body resting energy expenditure (A), RER (B), carbohydrate oxidation (C), and fat oxidation (D) during the awake period of day 4.

(E–G) Overview of 24-h plasma metabolites on day 4: plasma level of glucose (E), serum free fatty acids (F), and serum TAG (G). The dark gray area represents the sleeping period (23:00–07:00h).

(H–K) Whole-body resting energy expenditure (H), RER (I), carbohydrate oxidation (J), and fat oxidation (K) in response to the MMT on day 5. (L–O) Postprandial plasma metabolites: plasma level of glucose (L), serum insulin (M), serum free fatty acids (N), and serum TAG (O). Data are presented as mean \pm SEM. * $p < 0.05$ based on the Bonferroni post hoc test.

no differences (condition or interaction) in proximal and distal skin temperatures as well as the distal-proximal skin temperature gradient were found between light conditions

in only one of the two conditions; hence, these four individuals were excluded for comparing DLMO between the two light conditions. DLMO was not different between light conditions (Figures S8B–S8D).

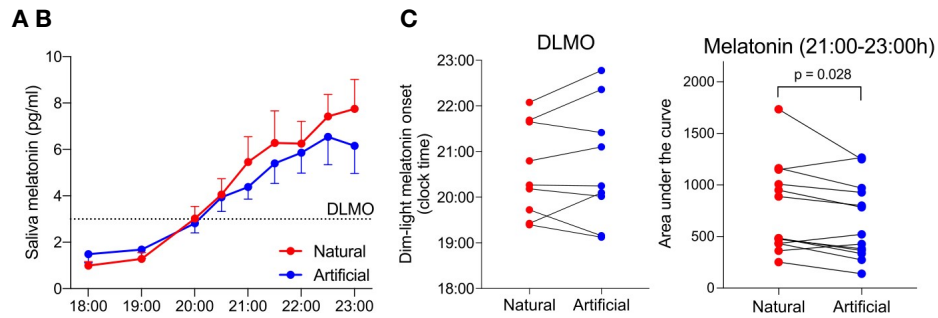
Higher late evening melatonin levels upon natural light but no differences in DLMO

Dim-light melatonin onset (DLMO) analysis revealed one individual that did not reach the threshold level of 3 pg/mL in both light conditions and three individuals that did not reach the threshold

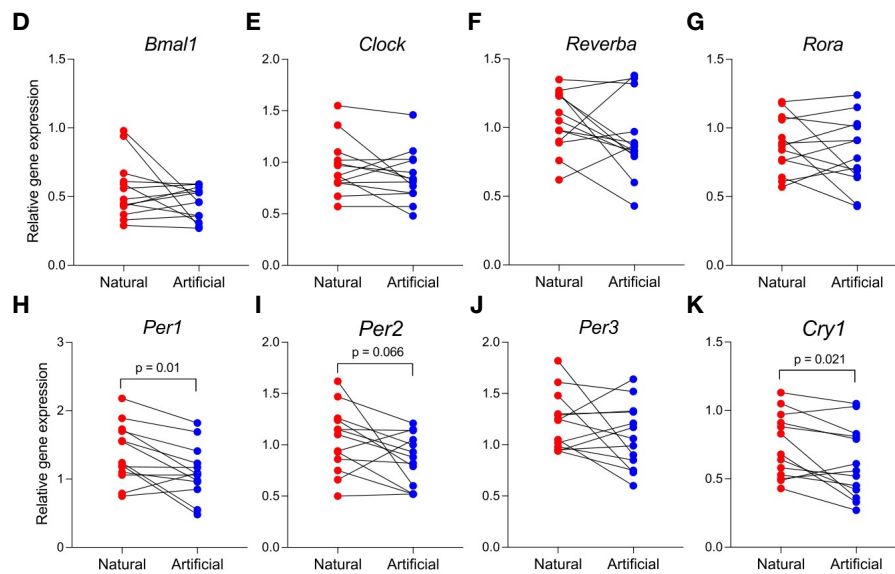
(mean \pm SD, natural, 20:35 \pm 01:01 h; artificial, 20:42 \pm 01:18 h, $p=0.47$, $n=9$; Figures 4A and 4B). However, melatonin

AUC from the average DLMO over both light conditions onward (21:00–23:00h) was higher in natural compared with artificial office light (natural, 755 ± 432 pg/mL \times min; artificial, 650 ± 374 pg/mL \times min, $p=0.029$, $n=13$; [Figure 4C](#)), indicating higher melatonin release after DLMO upon natural light.

Saliva melatonin levels in the evening (18:00-23:00h) of day 4:



Clock gene expression in skeletal muscle biopsies:



Molecular clockwork of human primary skeletal myotubes:

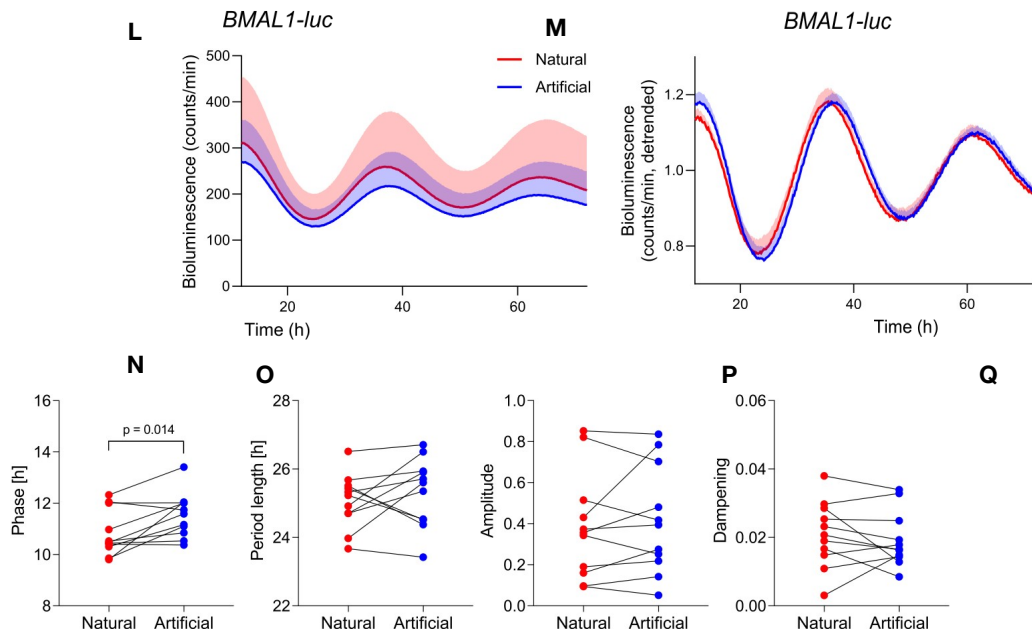


Figure 4. Evening melatonin levels and skeletal muscle clockwork

(A) Saliva melatonin levels were assessed in the evening (18:00–23:00h) of day 4 under dim-light conditions for both natural (red line) and artificial office lighting (blue line), and data are represented as mean \pm SEM.

Natural daylight may affect the molecular clocks operative in skeletal muscle of individuals with T2D, as measured in muscle biopsy and in primary myotubes synchronized *in vitro*

Paired *t* tests revealed no difference in mRNA levels of the core-clock genes *Bmal1*, *Clock*, *Reverba*, *Rora*, and *Per3* (Figures 4D–4J), assessed in skeletal muscle biopsies taken at a single time point on the morning of day 4, after an overnight fast. However, mRNA levels of the clock genes *Per1* (Figure 4H) and *Cry1* (Figure 4K) were higher upon natural light ($p=0.01$ and $p=0.021$, respectively), with a similar tendency for *Per2* ($p=0.066$; Figure 4I), suggesting that natural light may affect the muscle molecular clock. To investigate if these

S1), using shared and unique structures (SUSs) plot to visualize targets most strongly distinguishing between light conditions across both time points. Metabolomics analyses identified five key metabolites — threonine, cholic acid, uracil, erythro-dihydro-sphingosine, and glutamic acid — that exhibited the strongest positive associations with the natural light condition at both 08:00 and 16:00h (Figure 5A). The levels of these metabolites changes in components of the molecular clock measured in a single time-point muscle biopsy translate into altered clock rhythmicity in muscle, we next assessed molecular clock work in primary myotubes established from these skeletal muscle biopsies and differentiated *in vitro* using a *Bmal1-luc* reporter allowing for continuous measurement of the cellular clocks^{37,38} (Figures 4L and 4M). Of note, the phase of *Bmal1-luc* oscillations of primary skeletal myotubes established from biopsies taken after the natural light condition was 0.75 ± 1.03 h advanced compared with the artificial light regimen ($p=0.014$; Figure 4N; individual profiles are shown in Figure S9A). The period length ($p=0.87$; Figure 4O), amplitude ($p=0.79$; Figure 4P), and oscillation damping ($p=0.42$; Figure 4Q) were comparable between light regimens. Given that we detected light-induced alterations in both core-clock transcript status in muscle biopsies and the circadian phase of bioluminescence in cultured myotubes, we next investigated whether variations in muscle clock gene expression could infer myotube bioluminescence phase. Indeed, the muscle biopsy clock gene expression was able to predict the bioluminescence phase in

were consistently higher under natural light compared with artificial light at both time points, as seen in the box plots highlighting cholic and glutamic acid levels at both time points (Figure 5B). By contrast, hydroxyproline, allantoin, hydroxyphenylacetic acid, citric/isocitric acid, and salicylic acid were the top five metabolites showing the strongest negative association with natural light (Figure 5A).

Comparing the lipid families between light conditions revealed ether-linked phosphatidylethanolamine (PE-O), phosphatidylethanolamine (PE), diacylglycerol (DAG), and lysophosphatidylethanolamine (LPE) families as those bearing the highest positive association with the natural light condition (Figure 5C). On the other hand, glucosylceramides (GlcCer), ceramides (Cer), and cholesteryl esters (CEs) were the classes most negatively associated with natural light (Figure 5C). Individual box plots of these lipid families corroborate the findings of the DA, highlighted by an increase in PE-O and a tendency for myotubes with a Pearson correlation coefficient of $R=0.51$ ($p=0.016$) (Figures S9B and S9C), with *Cry1* and *Per3* having the largest positive and negative contributions to the estimated bioluminescence phase, respectively.

Differential impact of the lighting conditions on the multi-omic landscape in the circulation

Since natural light impacted metabolism differentially compared with artificial light, we next applied targeted serum metabolomics, lipidomics, and monocyte RNA-seq analysis to the blood samples obtained on day 4 at 08:00 (after the overnight fast, preceding the respective light exposure period) and 16:00h (at the end of the respective light exposure period). To identify targets associated with light-dependent biological differences, we applied orthogonal partial least squares discriminant analysis (OPLS-DA) to each dataset (metabolomics, lipid families, lipid species, and transcriptomics) at both 08:00 and 16:00h (Data

Figure 5D). Consistently, the SUS plot of individual lipid species shows LPE16:0, lysophosphatidylcholine (LPC)15:0, phosphatidylcholine (PC)38:6, PC37:6, and PE36:2 as most positively linked with the natural light condition at both time points (Figure 5E). Negative associations to the natural light condition were observed for CE18:1, PC38:2, PC35:5, CE16:1, and PC38:3. This is supported by box plots of two top lipid species (CE18:1 and LPE16:0) identified by the DA

(Figure 5F).

Further, we used a SUS plot to display monocyt transcripts most discriminating between the light conditions at each time point. This analysis revealed *LINC01134*, *MIR8085*, *FAM157A*, *TOB1-AS1*, and *MGC16142* as the transcripts most positively associated with natural light, and *NMB*, *REM2*, *CLDND2*, *MC1R*, and *CBX3P2* as the transcripts most negatively associated with the natural light condition (Figure 5G). These changes are highlighted by box plots displaying expression levels of two

genes, *REM2* and *NMB* (Figure 5H). To further investigate these transcriptional alterations, we conducted a gene set enrichment analysis (GSEA) and clustered and annotated the pathways revealing the greatest changes between light conditions (Data S2; Figures S10M and S10N). Top pathways were related to Cer and GlcCer regulation (Figures S10M and S10N); however, none reached statistical significance after false discovery rate (FDR) correction (Data S2). Volcano plots of the metabolomics,

(Band C) Individual data of DLMO; $n=9$ (B) and the area under the curve of melatonin levels ($n=13$) from 21:00 to 23:00h (C) are shown.

(D–K) Core-clock gene expression in the single skeletal muscle biopsy sample ($n=13$) collected between 07:30 and 08:30h on day 5 preceding the mixed meal test: individual mRNA levels of *Bmal1* (D), *Clock* (E), *Reverba* (F), *Rora* (G), *Per1* (H), *Per2* (I), *Per3* (J), and *Cry1* (K) are shown. Normalized expression levels were determined relative to the geometric mean of two housekeeping genes.

(L and M) Molecular clock oscillations in differentiated myotubes measured by BMAL1-luciferase reporter assay. Averaged profiles \pm SEM ($n=11$) shown as raw (L) and detrended (M) values for 12–72h after synchronization, and individual profiles on these outcomes are shown in Figure S9.

(N–Q) Circadian parameters of oscillation extracted from sinusoid fit generated by Chronostar 3.0 software: phase (N), circadian period length (O), amplitude (P), and oscillation damping (Q). Indicated p values were determined based on paired t tests.

OPEN ACCESS

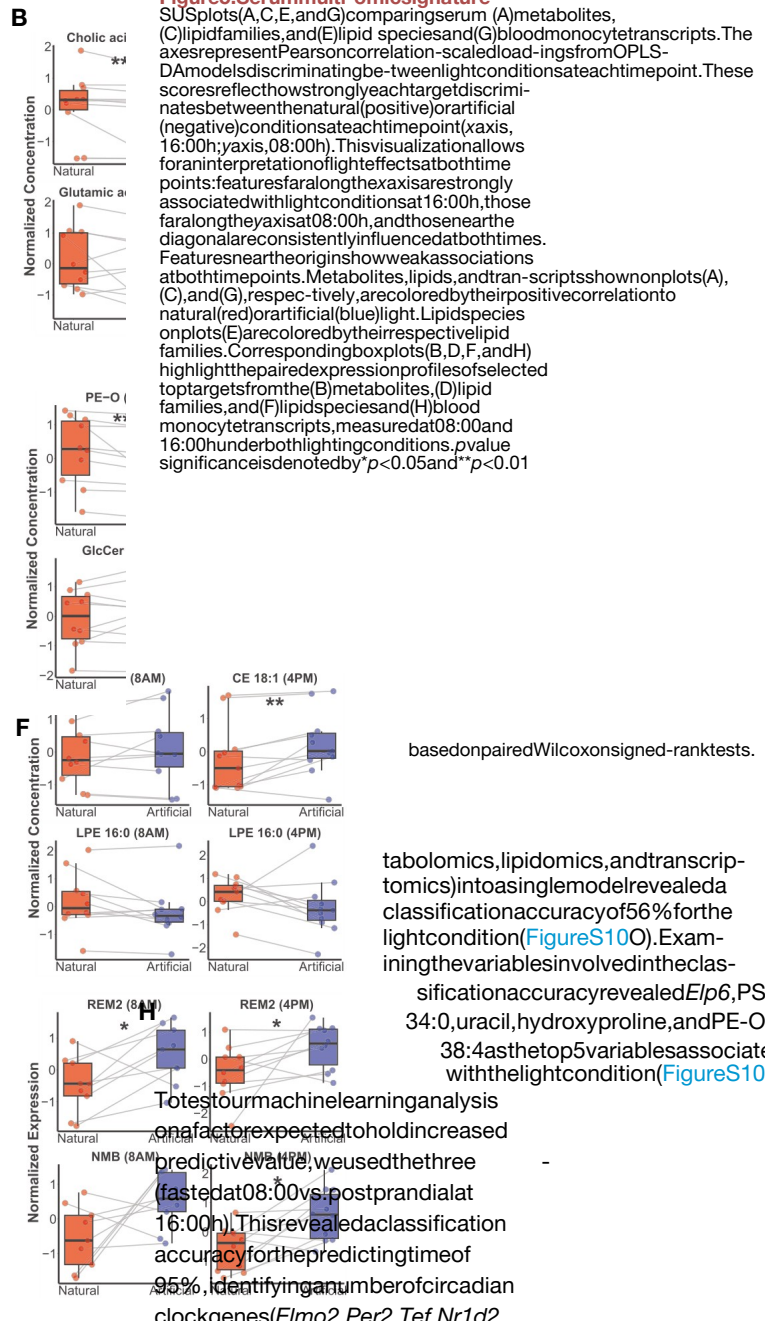
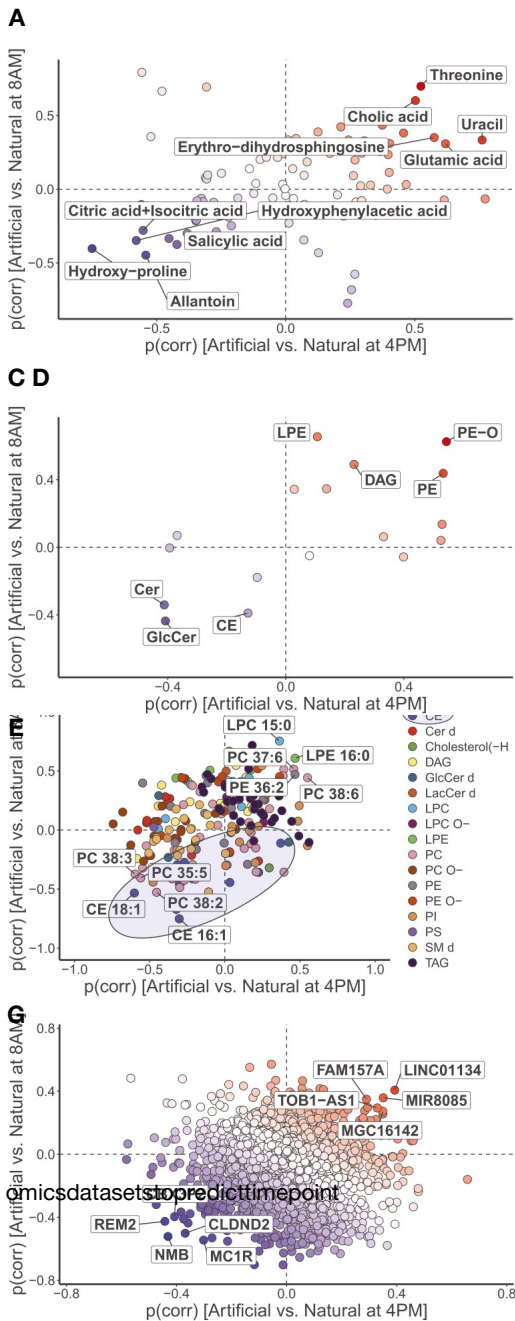


Figure 5. Serum multi-omics signature
 SUS plots (A, C, E, and G) comparing serum (A) metabolites, (C) lipid families, and (E) lipid species and (G) blood monocyte transcripts. The axes represent Pearson correlation-scaled loadings from OPLS-DA models discriminating between light conditions at each timepoint. These scores reflect how strongly each target discriminates between the natural (positive) or artificial (negative) conditions at each timepoint (x-axis, 16:00h; y-axis, 08:00h). This visualization allows for an interpretation of light effects at both time points: features far along the x-axis are strongly associated with light conditions at 16:00h, those far along the y-axis at 08:00h, and those near the diagonal are consistently influenced at both times. Features near the origin show weak associations at both time points. Metabolites, lipids, and transcripts shown on plots (A), (C), and (G), respectively, are colored by their positive correlation to natural (red) or artificial (blue) light. Lipid species on plots (E) are colored by their respective lipid families. Corresponding box plots (B, D, F, and H) highlight the paired expression profiles of selected top targets from the (B) metabolites, (D) lipid families, and (F) lipid species and (H) blood monocyte transcripts, measured at 08:00 and 16:00h under both lighting conditions. p-value significance is denoted by * $p < 0.05$ and ** $p < 0.01$

based on paired Wilcoxon signed-rank tests.

tabolomics, lipidomics, and transcriptomics) into a single model revealed a classification accuracy of 56% for the light condition (Figure S10O). Examining the variables involved in the classification accuracy revealed *Elp6*, *PS 34:0*, *uracil*, *hydroxyproline*, and *PE-O 38:4* as the top 5 variables associated with the light condition (Figure S10P).

To test our machine learning analysis on a factor expected to hold increased predictive value, we used the three (fasted at 08:00 vs. postprandial at 16:00h). This revealed a classification accuracy for the predicting time of 95%, identifying a number of circadian clock genes (*Elmo2*, *Per2*, *Tef*, *Nr1d2*, and *Per1*) along with deoxyribose, malic acid, and TAG species as carrying strong predictive value (Figure S10Q).

lipidomics, and transcriptomics, using a mixed model adjusting for time and participant ID as covariates, revealed no significant targets after FDR correction between natural and artificial light at 08:00, 16:00h, or in a comparison combining the two time points (Figures S10A–S10L).

Machine learning analysis classifying light and time conditions uncovers significant targets
 We applied a random-forest machine learning model to discover multivariate predictive factors that are not revealed in the univariate analysis. Merging the three datasets (i.e., me-

Time-of-day signature of blood metabolites, lipids, and monocyte transcripts
 Since diurnal rhythmicity of metabolic, lipid, and transcriptional

landscapes has been reported in human individuals, with differential temporal orchestration observed between individuals with T2D and normoglycemic counterparts, [11](#), [18](#), [39](#), [40](#) we zoomed into the temporal alterations associated with the applied light regimens. To this end, we compared the metabolite, lipid, and

transcript signatures between 08:00 and 16:00 h by pooling samples from the two light conditions. Serum metabolomics reveals 60 significantly altered metabolites between time points (Figure S11 A), with deoxyribose, proline, and malic acid as the most increased and hypoxanthine, ribose 5-phosphate, and xanthine as the most decreased metabolites at 16:00 h.

Analyzing differences in lipid families showed 5 significantly different classes between time points (Figure S11 B), with TAG and LPE highly increased at 16:00 h compared with 08:00 h. This is further supported by comparing individual lipid species between time points, revealing 8 TAG species as the most increased lipids at 16:00 h (Figure S11 C). Comparing differences in monocyte transcripts displayed 920 differential transcripts between time points, with *Elmo2*, *Per1*, *Per2*, *Reverb β* , *Tef*, *Flt3*, *Alas1*, *Lmo2*, *Mdm2*, and *Peli1* as the most significantly altered transcripts by p-value between time points (Figure S11 D). GSEA using the RNA-seq data revealed decreases in pathways related to mitochondrial membrane fission and the intrinsic apoptotic signaling pathway in response to hypoxia at the 16:00 h time point (Figure S11 E).

In line with previous studies,^{26,27} we found a tendency for a larger excursion in postprandial glucose upon natural light upon a fluid mixed meal challenge performed in the morning after the overnight fast. Intriguingly, though, the time spent in the normal glucose range across the 4.5-day intervention period was higher upon natural light (together with higher whole-body fat oxidation levels on day 4), suggesting improved glucose control in individuals with T2D upon longer-term natural light exposure. Hence, the potentially negative impact of (bright) light exposure on postprandial plasma glucose levels in the short term may be time-of-

DISCUSSION

Nowadays, almost 90% of our time is spent indoors,^{19–21} and during the daytime, we are thereby exposed to lower light intensities and a different wavelength spectrum from artificial light sources compared with natural daylight. Since light is the main *zeitgeber* for our circadian time-keeping system^{2–4} that can modulate human metabolism acutely in a time-of-day-dependent manner,^{26,27} chronic lack of natural daylight could be considered a risk factor in society's rising incidence of metabolic diseases. Therefore, in this study, we hypothesized that individuals with T2D would benefit from being exposed to natural daylight during office hours when compared with typical constant artificial lighting. Although the average interstitial glucose level was not different between office light conditions, we found that glucose control (i.e., % time spent in the normal glucose range: 4.4–7.2 mmol/L) was significantly improved during the 4.5 days of natural lighting. This was accompanied by lower whole-body carbohydrate oxidation and, conversely, higher fat oxidation rates during waking hours upon natural light, as measured on day 4. Consistent with the higher fat oxidation, plasma free fatty acid levels were higher upon a liquid mixed meal challenge in natural compared with artificial office lighting.

To date, a few clinical studies have shown that the intensity of environmental light during daytime can impact glucose control of individuals with T2D²⁶ and insulin resistance.²⁷ For instance, enhancing intensity levels of artificial light sources to a constant 1,250²⁷ or 4,000 photopic lux²⁶ during morning hours consistently led to elevated postprandial glucose levels following a morning meal after overnight fasting compared with 10 lux. Other studies,^{41,42} but not all,²⁶ reported similar effects in young individuals. Also, Mengetal. found reduced glucose tolerance in young healthy adults upon white light exposure of 400 lux compared with darkness applied both during daytime and nighttime.⁴² In this study, natural light encompassed diurnal changes in both light intensity and its wavelength spectrum (Figures 1C and 1D), whereas the control artificial light condition was more applicable to the real world (e.g., 300 lux) instead of dim light.

day dependent and should be investigated in future studies by administering the meal tests at different times of the day.

In a prospective cohort study, Lu et al. correlated all-cause mortality with the time spent in the normal glucose range and found that less time in the normal range was associated with a higher hazard ratio for all-cause mortality in individuals with T2D,⁴³ indicating that the time spent in the normal range is a clinically relevant outcome. Interestingly, time-restricted eating regimens in individuals with T2D have been shown to lower 24-h glucose levels and to increase the time spent in the normal range^{44,45} by 12% and 10%, respectively. The improvement in glucose control observed in this study is also in line with improvements seen in CGM profiles of individuals with T2D upon

both short- and long-term exercise programs.⁴⁶ Modeling the continuous glucose data revealed that natural light led to lower amplitudes of 24-h fluctuations in glucose levels, which were associated with more time spent in normal range across participants. This suggests that exposure to natural light may have a beneficial effect on 24-h glucose metabolism. Future studies should ascertain the molecular regulatory mechanisms underlying the observed beneficial effect of exposure to natural light on 24-h glucose rhythms.

Enhancing daytime light intensities has repeatedly been shown to increase nocturnal melatonin levels in young individuals,^{28,47,48} but cross-sectional associations between brighter daytime light and higher nocturnal melatonin levels were also found in the elderly.⁴⁹ In addition, natural daylight exposure throughout outdoor camping has been shown to induce consistent phase advances in DLMO in individuals.⁵⁰ We here demonstrate that in older individuals with T2D, both the nadir in CBT and DLMO were relatively stable irrespective of daytime office lighting, but melatonin levels were higher in the last 2 h before bedtime (21:00–23:00) upon exposure to natural light during the daytime, as compared with artificial lighting. An indication that the peripheral circadian system was modified through the differential office lighting was derived from the higher mRNA levels of several clock genes (i.e., *Per1-2* and *Cry1*) in skeletal muscle upon natural lighting. Subsequently, we investigated the rhythmic properties of myotubes generated from our participants after exposure to both office lighting regimes. Consistent with the effect of natural light on clock gene expression in the muscle biopsies, we found a phase advance in the rhythm of the *Bmal1*-luciferase reporter following natural light exposure. While the *in vitro* synchronization for forskolin pulse brings the individual cellular oscillator to the same initial phase, it does not alter the core-clock machinery *per se*.^{51,52} Thus, the phase advance persisted even though we synchronized the cultured myotubes, suggesting natural light may induce lasting changes to the core-clock feedback loop. Noteworthy, BMAL1 was

previously reported to impact glucose control in mice⁵³ and humans.⁵⁴ We also found that the muscle clock gene expression could be used to infer *in vitro* bioluminescence phase data, although this correlation warrants validation based on muscle biopsies from donors with T2D collected around the clock. We identified the core-clock genes *Cry1* and *Per3* as having the strongest influence on phase estimation. Elucidation of

workplace.⁶⁵ Similarly, mimicking natural daylight by dynamically changing the wavelength spectrum and the intensity of artificial indoor lighting across the day improves sleep latency.²⁸

the molecular mechanisms controlling the alterations of muscle clockwork upon natural light in individuals with T2D represents a promising direction for follow-up studies.

To further investigate the light-responsive circulating factors that may account for differences in glucose homeostasis, we compared the multi-omics signature in blood samples between light conditions. Our metabolomics analysis revealed an increase in cholic acid under natural light, consistent with previous findings identifying it as increased in duck exposed to 460 nm blue light, a wavelength exhibiting higher photon flux in the natural compared with the artificial light condition.⁵⁵ Glutamate levels were also elevated in natural light and have been reported as UV-responsive in murine brain tissue, particularly to UVB.⁵⁶ While participants were not exposed to UVB, shorter wavelengths present in natural light may similarly upregulate glutamate. Furthermore, increased threonine levels that we observed upon natural light, concomitant with the improved glucose control, are well in line with the reduced level of this amino acid in individuals with T2D that we extracted from a recently published serum metabolomics dataset.⁵⁷ Several lipid families also responded to light exposure. Notably, cholesterol esters and Cer negatively associated with natural light, aligning with previous reports of similar reductions in sterol esters and Cer in the human hair lipidome following exposure to 380 and 420 nm wavelengths.⁵⁸ Moreover, recent studies highlight Cer levels as increased in individuals with T2D.⁴⁰ Concordantly, we observed a trend toward reduced Cer upon natural light, corroborating improved glucose control. The transcriptomic analysis identified top pathways involved in the negative regulation of Cer and GlcCer, both of which were negatively associated with natural light in the lipidomics data. Additionally, LPEs, including LPE 16:0, particularly, were positively associated with natural light and have been linked to higher insulin sensitivity⁵⁹ and found to be decreased in serum from individuals with obesity.^{60,61} Together, these findings reveal a distinct multi-omics signature linked to natural light exposure, characterized by alterations in metabolites, lipids, and transcripts possibly underlying the improved glucose control.

Since sleep and overall physical activity levels can both have an impact on glucose homeostasis outcomes, we assessed these parameters as potential confounders. However, we could

Therefore, we cannot rule out that it improves sleep quality (partially) drives the metabolic benefits associated with the natural light exposure during daytime.

Future directions

We chose the strong contrast of dynamic natural light through a window vs. an artificial light condition that deprived participants of any enriched short-wavelength daylight throughout the 4.5-day study period as a proof of concept that natural light elicits distinct metabolic effects compared with artificial light only. Future studies could usefully explore if longer-term exposure to natural light could elicit more pronounced effects or if alternative strategies, such as natural light exposure during working commutes (e.g., before and/or after office hours, as is typically the case in the real world⁶⁶), would be sufficient to offset the negative effects of artificial lighting revealed in this study.

Limitations of the study

While our crossover design strengthens the reliability of our findings, one limitation of the study is the small sample size ($n=13$). Our finding of improved time in the normal glucose range (4.4–7.2 mmol/L) upon natural light may warrant cautious interpretation until more long-term clinical trials (e.g., exceeding 4.5 days up to weeks and months) confirm the clinical relevance through improvement of the TIR (3.9–10.0 mmol/L). Furthermore, the

not detect any differences between light conditions, neither prior to nor during the experimental period. Particularly, physical activity was highly standardized in this study by scheduled standing and stepping activity times. However, sleep outcomes were only assessed through subjective questionnaires and not quantified through more objective means, such as polysomnography (PSG). Compromised sleep is linked to impaired glucose control,⁶² and sleep loss has even been shown to modify skeletal muscle mRNA levels of *Bmal1* and *Cry1* as well as protein levels of BMAL1.^{63,64} Office workers in windowless environments reported poorer sleep scores than workers with windows at the

average age of our study population was 70 years, and 12 participants were at least 65 years old, which compromises the generalizability of our findings. Future studies could study the potential metabolic benefits of natural vs. artificial (office) lighting across a wider age range within the working population in real office environments. Furthermore, all experiments were conducted during Central European Summer Time (i.e., from April to October). Natural light varies strongly as a function of geographical location, weather, and season, where seasonal light changes can modulate energy metabolism and peripheral clocks in mice⁶⁷ and gene expression in humans.⁶⁸ Future studies are needed to establish how the effects size of the natural light intervention changes with the time of year and location. Finally, while our multivariate analyses identified targets differentiating natural and artificial light conditions at both time points, the models demonstrated limited predictive accuracy, likely due to the small sample size of this exploratory cohort. This underscores the need for further investigation into the mechanisms by which natural light influences metabolic health.

Conclusions

In conclusion, through comparing real-world office lighting scenarios of natural daylight through windows vs. constant artificial lighting in individuals with T2D, we found metabolic benefits associated with natural daylight exposure. Specifically, more time spent in the normal glucose range and a shift in whole-body substrate metabolism toward higher fat oxidation levels indicated improved glucose control upon natural lighting. Our findings provide a strong rationale for future research to focus more on the interaction of (natural) light exposure and metabolic health. This study also highlights the often-unnoticed impact of

Cell Metabolism

Article

the built environment on our health and raises further concerns about the prevalence of office environments with poor (natural) daylight access.



- **EXPERIMENTAL MODEL AND SUBJECT DETAILS**

- Participant recruitment

- **METHOD DETAILS**

- Sample size calculation

RESOURCE AVAILABILITY

Lead contact

Further information and requests for resources should be directed to and will be fulfilled by the lead contact, Joris Hoeks).

Materials availability

This study did not generate new, unique reagents.

Data and code availability

Metabolomics and lipidomics data supporting the findings of this study are available in DataS3. Raw RNA-seq data have been deposited in GEO under the accession number GEO:GSE309688. Any additional information required to analyze the data reported in this paper is available from the [lead contact](#) upon request.

ACKNOWLEDGMENTS

This study was supported by VELUX Stiftung (C.D. and J.H., project number 1471), grants from the Swiss National Science Foundation (310030-219187 to C.D. and PZ00P3-167826 and 32003B-212559 to T.-H.C.), the Vontobel Foundation (C.D. and T.-H.C.), the Olga Mayenfisch Foundation (C.D.), Ligue Pulmonaire Genevoise (C.D.), Swiss Cancer League (KFS-5266-02-2021-R; C.D.), the SREC Foundation (C.D.), the Gertrude von Meissner Foundation

- Study design
- Study meals

- Quantificationoflightcharacteristics
- Continuousglucosemonitoring
- Bodycomposition
- Sleepandmoodquestionnaires
- Indirectcalorimetry
- Ambient,skinandcorebodytemperature
- Bloodpressureandheartrateassessment
- 24-hourbloodandeveningsalivasampling
- Skeletalmusclebiopsy
- Mixedmealtolerancetest
- Salivarymelatoninassessment

(C.D.), the Swiss Life Jubiläumstiftung Foundation (T.-H.C. and A.D.B.), the Swiss Society of Endocrinology and Diabetes (T.-H.C. and N.E.P.), the Nutrition 2000 plus Foundation and the Medical Board of the Geneva University Hospitals (T.-H.C.), and the Hjeltn Foundation (N.E.P.). J.-F.H. was funded by the project "Profilbildung Built and Lived Environment" (PB22-062). The project "Profilbildung Built and Lived Environment" has received funding from the program "Profilbildung 2022," an initiative of the Ministry of Culture and

- Plasma, serum and monocyte analysis
- Serum mass spectrometry analyses
- Monocyte transcriptomic analyses
- Muscle gene transcript quantification
- Primary human skeletal myotube culture and lentiviral transduction
- Real-time bioluminescence recording and analysis

• QUANTIFICATION AND STATISTICAL ANALYSIS

SUPPLEMENTAL INFORMATION

Supplemental information can be found online at

Received: February 23, 2025
Revised: June 20, 2025

Science of the State of Northrhine Westphalia. The sole responsibility for the content of this publication lies with the authors. The authors are grateful to Ok-sana Fiammingo, Dylan Gendre, and the iGE3 genomics platform (University of Geneva) for their help with RNA isolation and sequencing procedures; to Marcel Schweiker for providing the handheld spectrometer device for the duration of the study; and to Chrono@Work for performing the melatonin analysis. The authors are thankful for the support provided by the Metabolomics Facility of the Molecular Discovery Platform at the CeMM Research Center for Molecular Medicine (Austrian Academy of Sciences) for mass-spectrometric data acquisition.

AUTHOR CONTRIBUTIONS

Conceptualization, J.-F.H., I.H., D.D., H.P., M.C.M.G., T.-H.C., A.K., P.S., C.D., and J.H.; methodology, J.-F.H., I.H., P.S., C.D., and J.H.; formal analysis, J.-F.H., I.H., A.D.B., A.L., N.E.P., L.M., and J.S.-A.; investigation, J.-F.H., I.H., A.D.B., A.L., N.E.P., L.M., J.S.-A., M.K., M.T., D.H., S.S.d.K., G.S., J.A.J., A.G., E.M.-K., T.v.d.W., M.B., F.H., R.D.L., and H.P.; writing—original draft, J.-F.H., I.H., A.D.B., A.L., J.H., P.S., C.D., and N.E.P.; writing—review and editing, all authors; visualization, J.-F.H., I.H., A.D.B., A.L., L.M., and N.E.P.; supervision, P.S., C.D., and J.H.; project administration, C.D. and J.H.; funding acquisition, C.D., J.-F.H., P.S., and J.H.

DECLARATION OF INTERESTS

The authors declare no competing interests.

REFERENCES

1. Roenneberg, T., and Merrow, M. (2005). Circadian clocks—the fall and rise of physiology. *Nat. Rev. Mol. Cell Biol.* 6, 965–971..
2. Reppert, S.M., and Weaver, D.R. (2002). Coordination of circadian timing in mammals. *Nature* 418, 935–941..
3. Foster, R.G., Hughes, S., and Peirson, S.N. (2020). Circadian photoentrainment in mice and humans. *Biology* 9, 180..
4. Panda, S. (2016). Circadian physiology of metabolism. *Science* 354, 1008–1015..
5. Gutierrez-Monreal, M.A., Harmsen, J.-F., Schrauwen, P., and Esser, K.A. (2020). Ticking for metabolic health: the skeletal-muscle clocks. *Obesity (Silver Spring)* 28, S46–S54..
6. Zhang, R., Lahens, N.F., Ballance, H.I., Hughes, M.E., and Hogenesch, J.B. (2014). A circadian gene expression atlas in mammals: implications for biology and medicine. *Proc. Natl. Acad. Sci. USA* 111, 16219–16224. .
7. Reinke, H., and Asher, G. (2019). Crosstalk between metabolism and circadian clocks. *Nat. Rev. Mol. Cell Biol.* 20, 227–241..
8. van Moorsel, D., Hansen, J., Havekes, B., Scheer, F.A.J.L., Joergensen, J.A., Hoeks, J., Schrauwen-Hinderling, V.B., Duez, H., Lefebvre, P.,

Schaper, N.C., et al. (2016). Demonstration of a day-night rhythm in human skeletal muscle oxidative capacity. *Mol. Metab.* 5, 635–645. <https://doi.org/10.1016/j.molmet.2016.05.003> .

9. Gabriel, B.M., Altintas, A., Smith, J.A.B., Sardon-Puig, L., Zhang, X.,

Basse, A.L., Laker, R.C., Gao, H., Liu, Z., Dollet, L., et al. (2021).

STAR METHODS

Detailed methods are provided in the online version of this paper and include the following:

- KEY RESOURCE TABLE

Disrupted circadian oscillations in type 2 diabetes are linked to altered

Cell Metabolism 38, 65–
81, January 6, 2026
77

rhythmic mitochondrial metabolism in skeletal muscle. *Sci. Adv.* 7, eabi9654.

10. Wefers, J., Connell, N.J., Fealy, C.E., Andriessen, C., de Wit, V., van Moorsel, D., Moonen-Kornips, E., Jørgensen, J.A., Hesselink, M.K.C., Havekes, B., et al. (2020). Day-night rhythm of skeletal muscle metabolism is disturbed in older, metabolically compromised individuals. *Mol. Metab.* 47, 101050.
11. Harsen, J.-F., van Weeghel, M., Parsons, R., Janssens, G.E., Wefers, J., van Moorsel, D., Hansen, J., Hoeks, J., Hesselink, M.K.C., Houtkooper, R.H., et al. (2022). Divergent remodeling of the skeletal muscle metabolome over 24 h between young, healthy men and older, metabolically compromised men. *Cell Rep.* 41, 111786.

23. Stothard, E.R., McHill, A.W., Depner, C.M., Birks, B.R., Moehlman, T.M., Ritchie, H.K., Guzzetti, J.R., Chinoy, E.D., LeBourgeois, M.K., Axelsson, J., et al. (2017). Circadian entrainment to the natural light-dark cycle across seasons and the weekend. *Curr. Biol.* 27, 508–513..
24. Santhi, N., Thorne, H.C., vander Veen, D.R., Johnsen, S., Mills, S.L., Hommes, V., Schlangen, L.J.M., Archer, S.N., and Dijk, D.-J. (2012). The spectral composition of evening light and individual differences in the suppression of melatonin and delay of sleep in humans. *J. Pineal Res.* 53, 47–59..
25. Fleury, G., Masi's-Vargas, A., and Kalsbeek, A. (2020). Metabolic implica-
12. Vetter, C., Dashti, H.S., Lane, J.M., Anderson, S.G., Schernhammer, E.S., Rutter, M.K., Saxena, R., and Scheer, F.A.J.L. (2018). Night shift work, genetic risk, and type 2 diabetes in the UK Biobank. *Diabetes Care* 41, 762–769..
13. Buchvold, H.V., Pallesen, S., Øyane, N.M.F., and Bjorvatn, B. (2015). Associations between night work and BMI, alcohol, smoking, caffeine and exercise – across-sectional study. *BMJ Public Health* 15, 1112. .
14. Wefers, J., van Moorsel, D., Hansen, J., Connell, N.J., Havekes, B., Hoeks, J., van Marken Lichtenbelt, W.D., Duez, H., Phielix, E., Kalsbeek, A., et al. (2018). Circadian misalignment induces fatty acid metabolism gene profiles and compromises insulin sensitivity in human skeletal muscle. *Proc. Natl. Acad. Sci. USA* 115, 7789–7794..
15. Scheer, F.A.J.L., Hilton, M.F., Mantzoros, C.S., and Shea, S.A. (2009). Adverse metabolic and cardiovascular consequences of circadian misalignment. *Proc. Natl. Acad. Sci. USA* 106, 4453–4458..
16. Morris, C.J., Yang, J.N., Garcia, J.I., Myers, S., Bozzi, I., Wang, W., Buxton, O.M., Shea, S.A., and Scheer, F.A.J.L. (2015). Endogenous circadian system and circadian misalignment impact glucose tolerance via separate mechanisms in humans. *Proc. Natl. Acad. Sci. USA* 112, E2225–E2234..
17. Petrenko, V., Gandasi, N.R., Sage, D., Tengholm, A., Barg, S., and Dibner, C. (2020). In pancreatic islets from type 2 diabetes patients, the dampened circadian oscillators lead to reduced insulin and glucagon exocytosis. *Proc. Natl. Acad. Sci. USA* 117, 2484–2495..
18. Petrenko, V., Sinturel, F., Loizides-Mangold, U., Montoya, J.P., Chera, S., Riezman, H., and Dibner, C. (2022). Type 2 diabetes disrupts circadian orchestration of lipid metabolism and membrane fluidity in human pancreatic islets. *PLoS Biol.* 20, e3001725..
19. Klepeis, N.E., Nelson, W.C., Ott, W.R., Robinson, J.P., Tsang, A.M., Switzer, P., Behar, J.V., Hern, S.C., and Engelmann, W.H. (2001). The National Human Activity Pattern Survey (NHAPS): a resource for assessing exposure to environmental pollutants. *J. Expo. Anal. Environ. Epidemiol.* 11, 231–252..
20. Matz, C.J., Stieb, D.M., Davis, K., Egyed, M., Rose, A., Chou, B., and Brion, O. (2014). Effect of age, season, gender and urban-rural status on time-activity: Canadian Human Activity Pattern Survey 2 (CHAPS2). *Int. J. Environ. Res. Public Health* 11, 2108–2124..
21. Schweizer, C., Edwards, R.D., Bayer-Oglesby, L., Gauderman, W.J., Ilacqua, V., Jantunen, M.J., Lai, H.K., Nieuwenhuijsen, M., and Ku'nzli, N. (2007). Indoortime-microenvironment-activity patterns in seven regions of Europe. *J. Expo. Sci. Environ. Epidemiol.* 17, 170–181..
22. Didikoglu, A., Mohammadian, N., Johnson, S., van Tongeren, M., Wright, P., Casson, A.J., Brown, T.M., and Lucas, R.J. (2023). Associations between light exposure and sleep timing and sleepiness while awake in a

tions of exposure to light at night: lessons from animal and human studies. *Obesity (Silver Spring)* 28, S18–S28..

26. Versteeg, R.I., Stenvers, D.J., Visintainer, D., Linnenbank, A., Tanck, M.W., Zwanenburg, G., Smilde, A.K., Fliers, E., Kalsbeek, A., Serlie, M.J., et al. (2017). Acute effects of morning light on plasma glucose and triglycerides in healthy men and men with type 2 diabetes. *J. Biol. Rhythms* 32, 130–142..
27. Harmsen, J.-F., Wefers, J., Doligeat, D., Schlangen, L., Dautzenberg, B., Rense, P., van Moorsel, D., Hoeks, J., Moonen-Kornips, E., Gordijn, M.C.M., et al. (2022). The influence of bright and dim light on substrate metabolism, energy expenditure and thermoregulation in insulin-resistant individuals depends on time of day. *Diabetologia* 65, 721–732..
28. Stefani, O., Freyburger, M., Veitz, S., Basishvili, T., Meyer, M., Weibel, J., Kobayashi, K., Shirakawa, Y., and Cajochen, C. (2021). Changing color and intensity of LED lighting across the day impacts on circadian melatonin rhythms and sleep in healthy men. *J. Pineal Res.* 70, e12714. .
29. Cajochen, C., Münch, M., Kobialka, S., Krauchi, K., Steiner, R., Oelhafen, P., Orguñal, S., and Wirz-Justice, A. (2005). High sensitivity of human melatonin, alertness, thermoregulation, and heart rate to short wavelength light. *J. Clin. Endocrinol. Metab.* 90, 1311–1316..
30. Hatori, M., Le, H., Vollmers, C., Keding, S.R., Tanaka, N., Buch, T., Waisman, A., Schmedt, C., Jegla, T., and Panda, S. (2008). Inducible ablation of melanopsin-expressing retinal ganglion cells reveals their central role in non-image-forming visual responses. *PLoS One* 3, e2451..
31. Gu'ler, A.D., Ecker, J.L., Lall, G.S., Haq, S., Altimus, C.M., Liao, H.-W., Barnard, A.R., Cahill, H., Badea, T.C., Zhao, H., et al. (2008). Melanopsin cells are the principal conduits for rod-cone input to non-image-forming vision. *Nature* 453, 102–105..
32. American Diabetes Association Professional Practice Committee (2022). 6. Glycemic targets: standards of medical care in diabetes-2022. *Diabetes Care* 45, S83–S96..
33. Seaquist, E.R., Anderson, J., Childs, B., Cryer, P., Dagogo-Jack, S., Fish, L., Heller, S.R., Rodriguez, H., Rosenzweig, J., and Vigersky, R. (2013). Hypoglycemia and diabetes: a report of a workgroup of the American Diabetes Association and the Endocrine Society. *Diabetes Care* 36, 1384–1395..
34. American Diabetes Association Professional Practice Committee (2024). 6. Glycemic goals and hypoglycemia: Standards of care in diabetes-2024. *Diabetes Care* 47, S111–S125..
35. American Diabetes Association Professional Practice Committee (2024). 7. Diabetes technology: Standards of care in diabetes-2024. *Diabetes Care* 47, S126–S144..
36. Phillips, N.E., Collet, T.-H., and Naef, F. (2023). Uncovering personalized glucose responses and circadian rhythms from multiple wearable biosensors with Bayesian dynamical modeling. *Cell Rep. Methods* 3, 100545. .

37. Petrenko, V., Saini, C., Perrin, L., and Dibner, C. (2016). Parallel measurement of circadian clock gene expression and hormone secretion in human primary cell cultures. *J. Vis. Exp.* 54673..
38. Perrin, L., Loizides-Mangold, U., Skarupelova, S., Pulimeno, P., Chanon, S., Robert, M., Bouzakri, K., Modoux, C., Roux-Lombard, P., Vidal, H., et al. (2015). Human skeletal myotubes display cell-autonomous circadian clock implicated in basal myokine secretion. *Mol. Metab.* 4, 834–845..
39. Dallmann, R., Viola, A. U., Tarokh, L., Cajochen, C., and Brown, S. A. (2012). The human circadian metabolome. *Proc. Natl. Acad. Sci. USA* 109, 2625–2629..
40. Sinturel, F., Chera, S., Brulhart-Meynet, M.-C., Montoya, J. P., Stenvers, D. J., Bisschop, P. H., Kalsbeek, A., Guessous, I., Jornayvaz, F. R., Philippe, J., et al. (2023). Circadian organization of lipid landscape is perturbed in type 2 diabetic patients. *Cell Rep. Med.* 4, 101299..
41. Cheung, J. N., Zee, P. C., Shalman, D., Malkani, R. G., Kang, J., and Reid, K. J. (2016). Morning and evening blue-enriched light exposure alters metabolic function in normal weight adults. *PLoS One* 11, e0155601..
42. Meng, J.-J., Shen, J.-W., Li, G., Ouyang, C.-J., Hu, J.-X., Li, Z.-S., Zhao, H., Shi, Y.-M., Zhang, M., Liu, R., et al. (2023). Light modulates glucose metabolism by a retina-hypothalamus-brown adipose tissue axis. *Cell* 186, 398–412. e17..

51. Balsalobre, A., Damiola, F., and Schibler, U. (1998). A serum shock inducible circadian gene expression in mammalian tissue culture cells. *Cell* 93, 929–937..
52. Balsalobre, A., Marcacci, L., and Schibler, U. (2000). Multiple signaling pathways elicit circadian gene expression in cultured Rat-1 fibroblasts. *Curr. Biol.* 10, 1291–1294..
53. Marcheva, B., Ramsey, K. M., Buhr, E. D., Kobayashi, Y., Su, H., Ko, C. H., Ivanova, G., Omura, C., Mo, S., Vitaterna, M. H., et al. (2010). Disruption of the clock components CLOCK and BMAL1 leads to hypoinsulinaemia and diabetes. *Nature* 466, 627–631..
54. Woon, P. Y., Kaisaki, P. J., Braganc, a, J., Bihoreau, M.-T., Levy, J. C., Farrall, M., and Gauguier, D. (2007). Aryl hydrocarbon receptor nuclear
43. Lu, J., Wang, C., Shen, Y., Chen, L., Zhang, L., Cai, J., Lu, W., Zhu, W., Hu, G., Xia, T., et al. (2021). Time in range in relation to all-cause and cardiovascular mortality in patients with type 2 diabetes: a prospective cohort study. *Diabetes Care* 44, 549–555..
44. Andriessen, C., Fealy, C. E., Veelen, A., van Beek, S. M. M., Roumans, K. H. M., Connell, N. J., Mevenkamp, J., Moonen-Kornips, E., Havekes, B., Schrauwen-Hinderling, V. B., et al. (2022). Three weeks of time-restricted eating improves glucose homeostasis in adults with type 2 diabetes but does not improve insulin sensitivity: a randomised crossover trial. *Diabetologia* 65, 1710–1720.
- translocator-like (BMAL1) is associated with susceptibility to hypertension and type 2 diabetes. *Proc. Natl. Acad. Sci. USA* 104, 14412–14417. .
55. Xia, D., Yang, L., Cui, J., Li, Y., Jiang, X., Meca, G., Wang, S., Feng, Y., Zhao, Y., Qin, J., et al. (2021). Combined analysis of the effects of exposure to blue light induces reveals a reduction in cholesterol accumulation through changes in methionine metabolism and the intestinal Microbiota. *Front. Nutr.* 8, 737059..
56. Zhu, H., Wang, N., Yao, L., Chen, Q., Zhang, R., Qian, J., Hou, Y., Guo, W., Fan, S., Liu, S., et al. (2018). Moderate UV exposure enhances learning and memory by promoting anovel glutamate biosynthetic pathway in the brain. *Cell* 173, 1716–1727. e17.

57. Du, N.-H., Sinturel, F., Nowak, N., Gosselin, P., Saini, C., Guessous, I., Jornayvaz, F.R., Philippe, J., Rey, G., Dermizakis, E.T., et al. (2024). Multi-omics correlates of insulin resistance and circadian parameters mapped directly from human serum. *Eur. J. Neurosci.* *60*, 5487–5504. .
59. Wilkin, C., Colonna, M., Dehaes, J., Esser, N., Iovino, M., Gianfrancesco, .
45. Parr, E.B., Steventon-Lorenzen, N., Johnston, R., Maniar, N., Devlin, B.L., Lim, K.H.C., and Hawley, J.A. (2023). Time-restricted eating improves measures of daily glycaemic control in people with type 2 diabetes. *Diabetes Res. Clin. Pract.* *197*, 110569.
58. Ross, A.B., Maes, E., Lee, E.J., Homewood, I., Marsh, J.M., Davis, S.L., and Willcut, R.J. (2022). UV and visible light exposure to hair leads to widespread changes in the hair lipidome. *Int. J. Cosmet. Sci.* *44*, 672–684..

- M.A., Fateur, M., Swinnen, J.V., Paquot, N., Piette, J., et al. (2021). New insights on the PBMC sphospholipidome in obesity demonstrate modulation associated with insulin resistance and glycemic status. *Nutrients* 13, 3461..
60. Jeziorny, K., Pietrowska, K., Sieminska, J., Zmyslowska-Polakowska, E., Munan, M., Oliveira, C.L.P., Marcotte-Chenard, A., Rees, J.L., Prado, C.M., Riesco, E., and Boule, N.G. (2020). Acute and chronic effects of exercise on continuous glucose monitoring outcomes in type 2 diabetes: a meta-analysis. *Front. Endocrinol.* 11, 495.

Kretowski, A., Ciborowski, M., and Zmyslowska, A. (2023). Serum metabolomics identified specific lipid compounds which may serve as markers

of disease progression in patients with Alstro' and Bardet-Biedl syndromes. *Front. Mol. Biosci.* *10*, 1251905.

47. Takasu, N. N., Hashimoto, S., Yamanaka, Y., Tanahashi, Y., Yamazaki, A., Honma, S., and Honma, K.-I. (2006). Repeated exposure to daytime bright light increases nocturnal melatonin rise and maintains circadian phase in young subjects under fixed sleep schedule. *Am. J. Physiol. Regul. Integr. Comp. Physiol.* *297*, R1799–R1807.

61. Tonks, K.T., Coster, A.C., Christopher, M.J., Chaudhuri, R., Xu, A., Gagnon-Bartsch, J., Chisholm, D.J., James, D.E., Meikle, P.J., Greenfield, J.R., et al. (2016). Skeletal muscle and plasma lipidomic signatures of insulin resistance and overweight/obesity in humans. *Obesity (Silver Spring)* 24, 908–916.
62. Reutrakul, S., and Van Cauter, E. (2014). Interactions between sleep, circadian function, and glucose metabolism: implications for risk and severity of diabetes. *Ann. N.Y. Acad. Sci.* 1311, 151–173.
49. Obayashi, K., Saeki, K., Iwamoto, J., Okamoto, N., Tomioka, K., Nezu, S., Ikada, Y., and Kurumatani, N. (2012). Positive effect of daylight exposure on nocturnal urinary melatonin excretion in the elderly: a cross-sectional analysis of the HEIJO-KYO study. *J. Clin. Endocrinol. Metab.* 97, 4166–4173.
50. Wright, K.P., Jr., McHill, A.W., Birks, B.R., Griffin, B.R., Rusterholz, T., and Chinoy, E.D. (2013). Entrainment of the human circadian clock to the natural light-dark cycle. *Curr. Biol.* 23, 1554–1558.

63. Cedernaes, J., Osler, M. E., Voisin, S., Broman, J. -E., Vogel, H., Dickson, S. L., Zierath, J. R., Schiøth, H. B., and Benedict, C. (2015). Acute sleep

loss induces tissue-specific epigenetic and transcriptional alterations to circadian clock genes in men. *J. Clin. Endocrinol. Metab.* *100*, E1255–E1261..

64.

Cell Metabolism, 38, 65–81, January 6, 2026

79

65. Boubekri, M., Cheung, I.N., Reid, K.J., Wang, C.-H., and Zee, P.C. (2014). Impact of windows and daylight exposure on overall health and sleep quality of office workers: a case-control pilot study. *J. Clin. Sleep Med.* *10*, 603–611.
66. Crowley, S.J., Molina, T.A., and Burgess, H.J. (2015). A week in the life of full-time office workers: workday and weekend light exposure in summer

[Neur1.6,795–802.](#)

81. van Marken Lichtenbelt, W.D., Daanen, H.A.M., Wouters, L., Fronczek, R., Raymann, R.J.E.M., Severens, N.M.W., and Van Someren, E.J.W. (2006).

Evaluation of wireless determination of skin temperature using iButtons. *Physiol. Behav.* *88*, 489–497.

and winter. *Appl. Ergon.* *46*, 193–200..

67. Small, L., Lundell, L.S., Iversen, J., Ehrlich, A.M., Dall, M., Basse, A.L., Dalbram, E., Hansen, A.N., Treebak, J.T., Barre's, R., et al. (2023). Seasonal light hours modulate peripheral clocks and energy metabolism in mice. *Cell Metab.* *35*, 1722–1735.e5..
68. Dopic, X.C., Evangelou, M., Ferreira, R.C., Guo, H., Pekalski, M.L., Smyth, D.J., Cooper, N., Burren, O.S., Fulford, A.J., Hennig, B.J., et al. (2015). Widespread seasonal gene expression reveals annual differences in human immunity and physiology. *Nat. Commun.* *6*, 7000..

82. Duffy, J.F., Dijk, D.J., Klerman, E.B., and Czeisler, C.A. (1998). Later

- endogenous circadian temperature and its relative to an earlier wake time in older people. *Am. J. Physiol.* 275, R1478–R1487..
83. Bergström, J., Hermansen, L., Hultman, E., and Saltin, B. (1967). Diet, muscle glycogen and physical performance. *Acta Physiol. Scand.* 71, 140–150..
69. Bueschl, C., Doppler, M., Varga, E., Seidl, B., Flasch, M., Warth, B., and Zanghellini, J. (2022). PeakBot: machine-learning-based chromatographic peak picking. *Bioinformatics* 38, 3422–3428..
70. Dobin, A., Davis, C. A., Schlesinger, F., Drenkow, J., Zaleski, C., Jha, S., Batut, P., Chaisson, M., and Gingeras, T. R. (2013). STAR: ultrafast universal RNA-seq aligner. *Bioinformatics* 29, 15–21..
71. Anders, S., Pyl, P. T., and Huber, W. (2015). HTSeq: a Python framework to work with high-throughput sequencing data. *Bioinformatics* 31, 166–169. .
72. Manders, R. J. F., Van Dijk, J.-W. M., and van Loon, L. J. C. (2010). Low-intensity exercise reduces the prevalence of hyperglycemia in type 2 diabetes. *Med. Sci. Sports Exerc.* 42, 219–225..
73. Harris, J. A., and Benedict, F. G. (1918). A biometric study of human basal metabolism. *Proc. Natl. Acad. Sci. USA* 4, 370–373..
74. Sparks, L. M., Moro, C., Ukropcova, B., Bajpeyi, S., Civitarese, A. E., Hulver, M. W., Thoresen, G. H., Rustan, A. C., and Smith, S. R. (2011). Remodeling lipid metabolism and improving insulin responsiveness in human primary myotubes. *PLoS One* 6, e21068.

85. StHilaire, M.A., and Lockley, S.W. (2022). Measuring dim light melatonin onset in humans. In *Melatonin. Methods and Protocols*, 2550, R. Jockers and E. Cecon, eds. (Springer), pp. 13–20..
86. Matyash, V., Liebisch, G., Kurzchalia, T.V., Shevchenko, A., and Schwudke, D. (2008). Lipid extraction by methyl-tert-butylether for high-throughput lipidomics. *J. Lipid Res.* 49, 1137–1146..
87. Loizides-Mangold, U., Perrin, L., Vandereycken, B., Betts, J.A., Walhin, P., Templeman, I., Chanon, S., Weger, B.D., Durand, C., Robert, M., J.-etal.
- (2017). Lipidomics reveals diurnal lipid oscillations in human skeletal muscle persisting in cellular myotubes cultured in vitro. *Proc. Natl. Acad. Sci. USA* 114, E8565–E8574..
88. Hannich, J.T., Loizides-Mangold, U., Sinturel, F., Harayama, T., Vandereycken, B., Saini, C., Gosselin, P., Brulhart-Meynet, M.-C., Robert, M., Chanon, S., et al. (2021). Ether lipids, sphingolipids and toxic deoxyceramides as hallmarks for lean and obese type 2 diabetic patients. *Acta Physiol. (Oxf.)* 232, e13610. 1-

75. CIE (2018). CIE S026/E:2018 CIE system for metrology of optical radiation

89. Robinson, M.D., McCarthy, D.J., and Smyth, G.K. (2010). edgeR: a Bioconductor package for differential expression analysis of digital gene expression data. *Bioinformatics* 26, 139–140.
76. Spitschan, M., Stefani, O., Blattner, P., Gronfier, C., Lockley, S.W., and Lucas, R.J. (2019). How to report light exposure in human chronobiology and sleep research experiments. *Clocks Sleep* 1, 280–289.
77. Plasqui, G., Soenen, S., Westerterp-Plantenga, M.S., and Westerterp, K.R. (2011). Measurement of longitudinal changes in body composition during weight loss and maintenance in overweight and obese subjects using air-displacement plethysmography in comparison with the deuterium dilution technique. *Int. J. Obes. (Lond)* 35, 1124–1130.

90. Reimand, J., Isserlin, R., Voisin, V., Kucera, M., Tannus-Lopes, C., Rostamianfar, A., Wadi, L., Meyer, M., Wong, J., Xu, C., et al. (2019). Pathway enrichment analysis and visualization of omics data using g:Profiler, GSEA, Cytoscape and EnrichmentMap. *Nat. Protoc.* *14*, 517..

78. Parrott, A.C., and Hindmarch, I. (1978). Factor analysis of a sleep evaluation questionnaire. *Psychol. Med.* *8*, 325–329..

79. Buysse, D.J., Reynolds, C.F., 3rd, Monk, T.H., Berman, S.R., and Kupfer,

91. Harmsen, J.-F., Kotte, M., Habets, I., Bosschee, F., Frenken, K., Jorgensen, J.A., de Kam, S., Moonen-Kornips, E., Cissen, J., Doligkeit, D., et al. (2023). Exercise training modifies skeletal muscle clock gene expression but not 24-hour rhythmicity in substrate metabolism of men with insulin resistance. *J. Physiol.* *602*, 6417–6433.

92. Hellemans, J., Mortier, G., DePaepe, A., Speleman, F., and Vandesompele, J. (2007). qBase relative quantification framework and D.J. (1989). The Pittsburgh Sleep Quality Index: a new instrument for psychiatric practice and research. *Psychiatry Res.* 28, 193–213..

software for management and automated analysis of real-time quantitative PCR data. *Genome Biol.* 8, R19.

94. Maier, B., Lorenzen, S., Finger, A.-M., Herzel, H., and Kramer, A. (2021). Searching novel clock genes using RNAi-based screening. *Methods Mol. Biol.* 2130, 103–114.

95. Bylesjö, M., Rantalainen, M., Cloarec, O., Nicholson, J.K., Holmes, E., and Trygg, J. (2006). OPLS discriminant analysis: combining the strengths of

PLS-DA and SIMCA classification. *J. Chemom.* 20, 341–351. <https://doi.org/10.1002/cem.1000>

96. Wiklund, S., Johansson, E., Sjöström, L., Mellerowicz, E.J., Edlund, U., Shockcor, J.P., Gottfries, J., Moritz, T., and Trygg, J. (2008). Visualization of GC/TOF-MS-based metabolomics data for identification

STAR METHODS

KEY RESOURCE TABLE

REAGENT or RESOURCE	SOURCE	IDENTIFIER
Biological samples		
Human blood samples	This study	N/A
Human saliva samples	This study	N/A
Human muscle biopsies samples	This study	N/A
Cultured human myotubes	This study	N/A
Chemicals, peptides, and recombinant proteins		
¹³ C2 Taurine	Cambridge Isotope Laboratories	CLM-6622-0.25
Labeled Amino Acid Mix	Cambridge Isotope Laboratories	MSKA2
LABELLED CARNITINE STANDARD SET B	Cambridge Isotope Laboratories	NSK-B
Fully ¹³ C-labelled Yeast Extract.	ISOTOPIC SOLUTIONS	¹³ C-labelled Yeast
CMP-lyophilized	JenaScience	NU-1032-5G
2'-Deoxycytidine(dC) freebase	JenaScience	N-1074-25G
2'-Deoxyguanosine monohydrate(dG)	JenaScience	N-DN-1003-25G
AMP-lyophilized	JenaScience	NU-1025-25G
dNTP Bundle 4x mM (dATP, dCTP, dGTP, dTTP)	JenaScience	NU-1005L
UMP-lyophilized	JenaScience	NU-1033-5G
(-)-Epicatechin	MetaSci	HMDB0001871
(+)-Pantothenic acid, sodium salt	MetaSci	HMDB0000210
2,2-Dimethylsuccinic acid	MetaSci	HMDB0002074
2,3-Dihydroxybenzoic acid	MetaSci	HMDB0000397
2,3-Pyridinedicarboxylic acid	MetaSci	HMDB0000232
2-Deoxyadenosine monohydrate	MetaSci	HMDB0000101
2-Amino-2-oxoacetic acid	MetaSci	PUBCHEM CID 974
2-Ketobutyric acid (liquid)	MetaSci	HMDB0000005
2-Oxo-3-phenylpropanoic acid	MetaSci	HMDB0000205
3-Hydroxybenzoic acid	MetaSci	HMDB0002466
3-Hydroxyphenylacetic acid	MetaSci	HMDB0000440
3-Methylglutaric acid	MetaSci	HMDB0000752
4-Aminobenzoic acid	MetaSci	HMDB0001392
4-Guanidinobutyric acid	MetaSci	HMDB0003464
4-Hydroxyphenylpyruvic acid	MetaSci	HMDB0000707
5-Hydroxyindole-3-acetic acid	MetaSci	HMDB0000763
5-Methoxytryptamine	MetaSci	HMDB0004095
6-Hydroxynicotinic acid	MetaSci	HMDB0002658
Adenosine 5'-triphosphate disodium salt	MetaSci	HMDB0000538
Adenosine cyclophosphate	MetaSci	HMDB0000058
Adipic acid	MetaSci	HMDB0000448
Allantoin	MetaSci	HMDB0000462
Amino adipic acid	MetaSci	HMDB0000510
Creatine anhydrous	MetaSci	HMDB0000064

Cytidine5-triphosphate(disodiumsalt)	MetaSci	HMDB000008 ₂
D-(-)-Quinicacid	MetaSci	HMDB000307 ₂
D-(+)-GalactosamineHCl	MetaSci	PUBCHEMCID7449 ₃
D-(+)-Ribono-1,4-lactone	MetaSci	HMDB000190 ₀
D-(+)-Xylose	MetaSci	HMDB000009 ₈

(Continuedonnextpage)

Continued

REAGENT or RESOURCE	SOURCE	IDENTIFIER
DL-6,8-Thioctamide/Lipoamide	MetaSci	HMDB000096
DL-Mevalonolactone	MetaSci	HMDB000602
D-Mannose	MetaSci	HMDB000016
FlavinAdenineDinucleotideDisodiumSalt	MetaSci	HMDB000124
Hydrate		
Folinicacidcalciumsalhydrate	MetaSci	HMDB000156
Guanosine5'-triphosphatesodiumsalt	MetaSci	HMDB000127
hydrate		
Hypoxanthine	MetaSci	HMDB000015
Indole-3-aceticacid	MetaSci	HMDB000019
Indole-3-ethanol	MetaSci	HMDB000344
Indoline-2-carboxylicacid	MetaSci	PUBCHEMID86074
Inosine	MetaSci	HMDB000019
Inosine5'-triphosphatetrisodiumsalt	MetaSci	HMDB000018
Inosine-5'-monophosphatesodiumsalt hydrate	MetaSci	HMDB000017
IsoamylAcetate(liquid)	MetaSci	HMDB003152
L-(-)-GlycericacidHemicalciumsalt(liquid)	MetaSci	HMDB000013
L-(-)-Malicacid	MetaSci	HMDB000015
L-Arabinose	MetaSci	HMDB000064
L-Arabitol	MetaSci	HMDB000185
L-Glutathioneoxidized	MetaSci	HMDB000333
L-Homoserine	MetaSci	HMDB000079
L-Hydrooroticacid	MetaSci	HMDB000052
L-Sorbose	MetaSci	HMDB000126
Malonicacid	MetaSci	HMDB000069
N-Acetyl-D-galactosamine	MetaSci	HMDB000021
N-Acetylglutamicacid	MetaSci	HMDB000113
N-Acetylneuraminicacid	MetaSci	HMDB000023
NAD	MetaSci	HMDB000090
N-Carbamyl-L-GlutamicAcid	MetaSci	HMDB006279
Nicotinicacid	MetaSci	HMDB000148
O-Phosphorylethanolamine	MetaSci	HMDB000022
Oroticacidanhydrous	MetaSci	HMDB000026
Phospho(enol)pyruvicAcid	MetaSci	HMDB000026
MonopotassiumSalt		
Phosphoserine	MetaSci	HMDB000027
Pyridoxal5'-phosphatehydrate	MetaSci	HMDB000149
Pyridoxalhydrochloride	MetaSci	HMDB000154
Pyridoxamine2HCl	MetaSci	HMDB000143
PyridoxineHCl	MetaSci	HMDB000023

Riboflavin	MetaSci	HMDB000024
Salicylicacid	MetaSci	HMDB000189
Shikimicacid	MetaSci	HMDB000307
Sodiumcreatinephosphatedibasic tetrahydrate	MetaSci	HMDB000151
SodiumD-gluconate	MetaSci	HMDB000062
Sodiumpyruvate	MetaSci	HMDB000024
TaurocholicAcid(sodiumsalt)	MetaSci	HMDB000003
Thiaminehydrochloride	MetaSci	HMDB000023
trans,trans-MuconicAcid	MetaSci	HMDB000234

(Continuedonnextpage)

Continued

REAGENT or RESOURCE	SOURCE	IDENTIFIER
trans-Aconitic acid	MetaSci	HMDB0000958
Uric acid	MetaSci	HMDB0000289
Vanillic acid	MetaSci	HMDB0000484
Xanthine	MetaSci	HMDB0000292
Xanthosine	MetaSci	HMDB0000299
Xylitol	MetaSci	HMDB0002917
7,8-Dihydrofolic acid	schirckslaboratories	16.206_50mg
(6R,S)-5,10-Methenyl-5,6,7,8-tetrahydrofolic acid chloride	schirckslaboratories	16.23_50mg
(6R,S)-5-Methyl-5,6,7,8-tetrahydrofolic acid, calcium salt	schirckslaboratories	16.235_50mg
2'-Deoxyadenosine 5'-monophosphate	Sigma	D6375-100MG
(±)-Sodium 2,3-dihydroxyisovalerate hydrate, ≥95% (CE)	Sigma	39693-10MG
(4R)-4-Hydroxy-L-glutamic acid, ≥98.0% (TLC)	Sigma	76157-10MG
(S)-Mevalonic acid lithium salt	Sigma	44714-10MG
13C1015N5AMP	Sigma	650676-1MG
13C1015N5dAMP	Sigma	900386
13C2 Citric acid	Sigma	488607-100mg
13C515N1 Folic acid	Sigma	803162-1MG
13C915N2UMP	Sigma	651370-1MG
2'-Deoxycytidine 5'-monophosphate sodium salt	Sigma	D7625-100MG
2-Deoxyuridine 5'-triphosphate Lithium	Sigma	1.142E+10
2-Deoxyribose 5-phosphate sodium salt, ≥95%	Sigma	D3126-25MG
3-Dehydroshikimic acid, ≥95.0% (HPLC)	Sigma	05616-10MG
4-Pyridoxic acid, ≥98%	Sigma	P9630-25mg
5-Deoxy-5-(methylthio)adenosine	Sigma	D5011-25MG
AlCAR (5-Aminoimidazole-4-carboxamide 1-β-D-ribofuranoside), ≥98% (HPLC), powder	Sigma	A9978-5MG
Amino acid standards, physiological	Sigma	A6407-10ML
Argininosuccinic acid disodium salt hydrate, ≥80%	Sigma	A5707-10MG
cis-Aconitic acid, ≥98%	Sigma	A3412-1G
D-(-)-Citramalic acid lithium salt, ≥95.0% (GC)	Sigma	06711-10MG
D-erythro-Dihydrosphingosine, ≥98%	Sigma	D3314-10MG
Dihydroxyacetone phosphate lithium salt, ≥95.0% (TLC)	Sigma	37442-100MG
D-Sedoheptulose 7-phosphate lithium salt, ≥90% (TLC)	Sigma	78832-1MG

D-Xylulose5-phosphatelithium salt_≥90%(TLC)	Sigma		15732-1MG
Folicacid<97%	Sigma	F7876-1G	
gamma-Glu-Cys_≥80%(HPLC)	Sigma	G0903-25MG	
Guanosine3,5-cyclic	Sigma	G7504-5MG	
monophosphate_≥98%(HPLC),powder			
L-2-Phosphoglycericaciddisodiumsalt hydrate_≥80%(CE)	Sigma		19710-50MG

(Continuedonnextpage)

Continued

REAGENT or RESOURCE	SOURCE	IDENTIFIER
N-Acetyl- α -D-glucosamine 1-phosphate	Sigma	A2142-5MG
disodiumsalt_>95%		
Prephenicacidbariumsalt_>75%	Sigma	P2384-10MG
S-5-Adenosyl-L-homocysteine_crystalline	Sigma	A9384-10MG
Sodium(\pm)-homocitratetribasic	Sigma	48488-10MG
Uridine5-diphosphoglucosedisodium	Sigma	94335-100MG
salt_>98.0%(HPLC)		
α -D(+)-Mannose 1-phosphatesodiumsalt hydrate_SigmaGrade	Sigma	M1755-10MG
α -D-Glucoheptonicacidsodiumsalt_	Sigma	G3516-100G
α -Ketoglutaricacid,>99.0%(T)	Sigma	75890-25G
2'-Deoxyinosine	Sigma	D5287-100MG
2-Isopropylmalicacid	Sigma	333115-100MG
Cystathionine	Sigma	C3633-100MG
D-Fructose 1,6-bisphosphatetrisodiumsalt hydrate	Sigma	F6803-10MG
D-Glucosamine 6-phosphate	Sigma	G5509-10MG
D-Ribose 5-phosphatedisodiumsalt hydrate	Sigma	R7750-10MG
L-Canavaninesulfatesalt	Sigma	C9758-100MG
Sodium L-lactate	Sigma	71718-10G
UDP- α -D-Galactose, Disodium Salt-CAS	Sigma	670111-M
137868-52-1-Calbiochem		
Ureidosuccinicacid	Sigma	69037-100MG
α -D-Glucose 1-phosphatedisodiumsalt hydrate	Sigma	G7000-1G
α -Hydroxyhippuricacid	Sigma	223875-5G
C18:1GlucoylCeramide-d5	AVANTI POLAR LIPIDS	860673
SPLASH LIPID MIX	AVANTI POLAR LIPIDS	330707
15:0-18:1(d7)PC	AVANTI POLAR LIPIDS	791637
15:0-18:1(d7)PE	AVANTI POLAR LIPIDS	791638
15:0-18:1(d7)PS	AVANTI POLAR LIPIDS	791639
15:0-18:1(d7)PG	AVANTI POLAR LIPIDS	791640
15:0-18:1(d7)PI	AVANTI POLAR LIPIDS	791641
15:0-18:1-d7-PA	AVANTI POLAR LIPIDS	791642
18:1(d7)LPC	AVANTI POLAR LIPIDS	791643
18:1(d7)LPE	AVANTI POLAR LIPIDS	791644
18:1-d7-cholesterol	AVANTI POLAR LIPIDS	791645
18:1(d7)MG	AVANTI POLAR LIPIDS	791646
15:0-18:1(d7)DG	AVANTI POLAR LIPIDS	791647
15:0-18:1(d7)-15:0TG	AVANTI POLAR LIPIDS	791648
18:1(d9)SM	AVANTI POLAR LIPIDS	791649
Cholesterol(d7)	AVANTI POLAR LIPIDS	700041
Critical commercial assays		
RNeasy tissue kit	Qiagen	74104
High capacity RNA-to- cDNA kit	ThermoFisher	4387406

Deposited data

Raw RNA-Seq data		GSE309688
Raw Metabolomic Data	This Study	DataS3
Raw Lipidomic Data	This Study	DataS3

(Continued on next page)

Continued

REAGENT or RESOURCE

SOURCE

IDENTIFIER

Software and algorithms

R (v4.5.0)

CRAN

TraceFinder 4.1

ThermoFisherScientific

PeakBot (v0.9.54)

Bueschletal.⁶⁹

Version 0.9.54

FastQC (v0.11.9)

BabrahamBioinformatics

Version 0.11.9

STARaligner (v2.7.0f)

Dobinetal.⁷⁰

Version 2.7.0f

HTSeq (v0.9.1)

Andersetal.⁷¹

Version 0.9.1

edgeR (v3.38.4)

Bioconductor (R)

Version 3.38.4

clusterProfiler (v4.9.0)

Bioconductor (R)

Version 4.9.0

org.Hs.eg.db (v3.15.0)

Bioconductor (R)

Version 3.15.0

limma (v3.58.1)

Bioconductor (R)

Version 3.58.1

Other

VanquishUHPLCsystem

ThermoFisherScientific

Orbitrap-based mass spectrometer

Fusion Lumos, ThermoFisherScientific

Accucore C18

ThermoFisherScientific

17126-152130

EXPERIMENTAL MODEL AND SUBJECT DETAILS

Participant recruitment

Men and postmenopausal women with type 2 diabetes (T2D), aged between 40 and 75 years, were recruited through advertisements in the vicinity of Maastricht. Participants were included if they were diagnosed with T2D for at least one year and were well controlled with respect to glycaemic control and stable diabetes medication regimens (more information in Table 1). Furthermore, participants needed to have stable body weight (no gain or loss of >5 kg in the last three months), a BMI of ≥ 25 kg/m², a regular sleep pattern (7–9 h/night) and a habitual bedtime of 23:00 ± 02:00 h. Participants were excluded if they were on sodium-glucose transport protein 2 (SGLT2) inhibitors or insulin treatment. Other exclusion criteria were uncontrolled hypertension, any other diabetes-related comorbidities like active cardiovascular disease, active diabetic foot, polyneuropathy or retinopathy, and active liver or kidney malfunctions. Extreme morning or evening chronotypes based on the MEQ-SA questionnaire (score of ≤ 30 for extreme evening or ≥ 70 for extreme morning type), shift work or travel across more than one time zone in the three months prior to the study and heavily varying sleep-wakerhythms were reasons for exclusion. Additional exclusion criteria were frequent engagement in programmed exercise, alcohol consumption of >2 servings per day for men and >1 serving per day for women, significant food allergies that hamper study participation, participants who did not want to be informed about unexpected medical findings, previous enrolment in a clinical study with an investigational product during the last 3 months, and smoking in the last six months. In- and exclusion criteria were assessed by a screening visit during which basic physical examination was performed (age, height, weight, and blood pressure), a fasting blood sample was obtained, and questionnaires were gathered. The overall eligibility of participants to be able to participate in the study was always assessed by a medical doctor. The study was executed in accordance with the declaration of Helsinki and was approved by the medical ethical committee of the Maastricht University Medical Center. The current study was registered at ([www.clinicaltrials.gov](#)) with the identifier NCT05263232. All participants provided written informed consent. The experiments took place between April and October 2022 to avoid confounding by the transition from European daylight-saving time to standard time and its associated change in photoperiod.

METHOD DETAILS

Sample size calculation

We hypothesized that natural office lighting during the day would improve average 24 h glucose levels compared to artificial office light. A previous trial investigating the effect of a nudge about to flow-intensity exercise on average 24-hour glucose levels [72](#) found a reduction of glucose levels from 9.4 ± 0.8 mmol/L to 7.8 ± 0.9 mmol/L (mean \pm SEM) corresponding to a mean change of $\sim 17\%$. We expected a potentially beneficial effect of natural daylight vs. artificial light to be less pronounced compared to the effect of low-intensity exercise and estimated that effect to be 10%. To estimate the required group size (n) we used the G*Power calculator [3.1](#) for a study design with two dependent samples (matched pairs, two-sided t-test). We assumed a $\sim 12\%$ between-subject variability of the change in average 24 h glucose measured by CGM, based on the aforementioned study, [72](#) with a power (1- β) of 80% and a significance level (α) of 5%, the sample size needed for our study was 14. The study was prematurely terminated after 13 completed participants, since we could only test that many participants over the summertime (April to October 2022) before the transition from daylight saving time to standard time occurred. In the Netherlands, the photoperiod progressively decreases from that point on, so that the artificial light condition would have been brighter than the natural light condition at the beginning and at the end of office hours. Furthermore, the office environment was no longer available from April 2023 onwards.

Study design

Randomization and allocation of eligible participants to the order of the two light conditions were carried out by sequential numbering (7 participants started with natural light as their first intervention period, and 6 participants vice versa). A washout of at least four weeks was kept between intervention periods. During the 3-day run-in period at home, participants were instructed to go to bed at 23:00 \pm 00:30 h and wake up at 07:00 \pm 00:30 h, avoid the consumption of caffeine and alcohol, follow a normal eating pattern (3 meals a day at regular times: 09:00, 14:00 and 19:00 \pm 00:30 h), refrain from strenuous exercise and avoid excessive bright or dim light during the day. A sleep and food diary were provided to participants to monitor similar behavior for both respective run-in periods. Adherence to the activity and bed times at home was further monitored using wrist-worn actigraphy (Actiwatch Spectrum Plus, Philips Respironics, Inc; Murrysville, PA, USA). In the morning between 07:00 and 08:00 h of day 2 to 5, participants stayed in artificial indoor lighting of < 400 lux (see more details below in the section “[quantification of light characteristics](#)”) and had the opportunity to take a shower. Room temperature was monitored every day during office lighting hours.

Study meals

During the intervention periods, participants were provided with standardized meals matching their energy requirements at fixed times. For this purpose, energy requirements were estimated based on the Harris-Benedict formula [73](#) multiplied with an activity factor of 1.5. Breakfast was served at 9:00 h and consisted of $\sim 21\%$ of the estimated daily energy intake (E%). Lunch was served at 14:00 h ($\sim 30\%$) and dinner was served at 19:00 h ($\sim 49\%$). Breakfast and lunch were bread-based, while the dinner mainly consisted of a pre-packaged meal. No other snacks or drinks were provided between meals except for water and decaffeinated tea or coffee. Daily macronutrient composition was aimed to resemble the typical Western diet with $\sim 31\%$ of the daily intake from fats ($\sim 9\%$ energy from saturated), $\sim 55\%$ from carbohydrates and $\sim 14\%$ from proteins. Identical meals were served for breakfast and lunch each day, while the type of dinner meal changed between days. Nonetheless, the overall meal plan was kept identical for both 4.5-day intervention periods. Participants maintained their diabetes medication schedule of ingesting respective pills concurrently with meals. To standardize physical activity, participants performed some light physical exercise for 30 min (e.g. 3x5 min of stepping on a single stair interspersed with 5 min of standing) three times per day, one hour after each meal.

Quantification of light characteristics

Light characteristics in the natural office light condition were measured at regular intervals each day during office hours (e.g. at 08:00, 10:00, 12:30, 14:00, 15:30 and 17:00 for day 1 to day 4; at 09:00, 10:00, 11:00, 12:00 and 13:00 on day 5 during the mixed meal tolerance test) with a spectrometer (Ai101 Spectral Irradiance Meter, Apacer, Taiwan). Artificial light sources were set up to achieve a light intensity of approximately 300 lux photopic illuminance (± 5 lux), which was monitored only once daily due to the constant nature of this light condition. On all occasions that participants had to leave the office room of their respective light condition or could be exposed to outdoor light or too bright light in the evening when going to the toilet, orange-tinted blue-light blocking glasses ([Figure S12A](#)) were worn. By using these orange-tinted blue-light blocking glasses, we ensured that throughout the 4.5-day study period in the artificial light condition the participants' eyes were never exposed to the enriched short-wavelengths of daylight, which are the wavelengths to which the human circadian system is most sensitive. To not induce any effect of using these orange-tinted blue-light blocking glasses only in the artificial light condition, participants also wore these glasses at the same instances in the natural light condition, whenever leaving the controlled office light environment. In both light conditions, between 07:00 and 08:00 as well as 17:00 and 18:00 h, participants stayed in indoor lighting conditions of < 400 lux. Subsequently, from 18:00 h to bedtime at 23:00 h, participants stayed in dim light conditions (< 5 lux) and the television and other electric devices were also set to < 5 lux. Nights were spent in complete darkness from 23:00 to 7:00 h.

All spectrometer measurements were carried out vertically in the outward direction of the optical axis at the eye levels simulating participants sitting at the office desks either facing the window (in natural office light), the wall (in artificial office light), or the television in the evening in dim light (for both light interventions), or the computer when sitting at the desk and once facing the TV sitting in bed

(see [Figure S12B](#) for a photo of the evening room). These latter two positions were selected as volunteers usually spent most of their time in the evenings in this manner of directing their view. The collected data were extracted and further converted from relative to absolute irradiance values by ⁷⁴Average illuminance, ⁷⁵opic (ir) radiances and spectral irradiances for the natural office light from day 1 to day 4 overall participants are reported according to Spitschan et al. ⁷⁶ in [Table S1](#). Similarly, light specifications for the time periods outside of office hours (e.g. 07:00–08:00, 17:00–18:00 and 18:00–23:00h) are reported in [Table S2](#). Only fluorescent light sources were installed in the respective laboratory rooms.

On day 3, participants stayed in a respiration chamber from 18:00 to 07:15 the next morning. From 18:00 to 23:00, dim light (<5 lux) was switched on, and during the dark sleeping period, participants could only switch on this dim light, when going to the toilet within the respiration chamber. The installed light system within the respiration chamber consisted of light-emitting diode (LED) wall washers (Philips Sky Ribbon IntelliHue Wall Washing Powercore). By combining and precisely controlling multiple channels of the LED light, the system can produce white light. The described dim light condition was set to a correlated colour temperature of 4000 K. Detailed spectral properties of the dim light condition within the respiration chamber were similar as reported previously ²⁷ and can be accessed using (under “Related Items”, photos of the spectral measurement set-up in [Figures S12C and S12D](#)).

Continuous glucose monitoring

After arrival on day 1 of each intervention period, a continuous glucose monitor (CGM) (Freestyle Libre Pro IQ, Abbott Laboratories, USA) was placed on the dominant upper arm of the participants. Interstitial glucose levels were measured every 15 minutes across the entire intervention period. Data of the CGM were not shown to the participants during the study. The CGM was removed at the end of the intervention period on day 5. To quantify the primary outcome of this study, namely glucose control, continuous glucose monitor data was obtained over the entire experimental period spent in the research facilities of 4.5 days for both natural and artificial office lighting. These continuous data were divided into categories based on the 2022 clinical practice recommendations of the American Diabetes Association (ADA), ³² which were available when our study was commenced: hypoglycemia <4.0 mmol/l, low blood glucose 4.0–4.3 mmol/l, normal range 4.4–7.2 mmol/l, high blood glucose 7.3–9.9 mmol/l, and hyperglycemia >10.0 mmol/l. Results are reported as percentages of times spent in the respective categories. Time in normal range (TIR) was also calculated according to the most recent (2024) recommendations of the ADA. ³⁵

To generate deeper insights into 24-hour glucose dynamics between light conditions, we further modelled the CGM data using a computational framework, ³⁶ taking the recurring standardized meal times (e.g. 09:00, 14:00 and 19:00h) into account. In brief, the meal times are used to model postprandial interstitial glucose increases, and both the size of the glucose spike (termed “response heights”) as well as the time needed for glucose to return to baseline (termed “response half-life”) are inferred for each individual and each light condition independently. The model also includes an underlying 24-hour cosinor function to describe 24-hour oscillations in baseline (i.e. irrespective of meal intake) glucose levels. This 24-hour cosinor function is described by “baseline”, “peak-to-trough amplitude” and “peak time” parameters, which are similarly learnt for each participant and light condition. The model is trained by minimizing the error between the model and the CGM data using a maximum a posteriori probability (MAP) estimate from 200 different starting conditions, and the settings and parameters of the original method were left unchanged. Associations between classic and modelled CGM parameters were quantified by combining the natural and artificial light conditions and using a linear mixed regression model accounting for repeated data in individual participants. The model was fitted using the “MixedLM” class from the “statsmodels” library (v0.13.0).

Body composition

To monitor if body composition remained stable over the washout period between light conditions, body composition was determined in the fasted state in the morning of day 2 of each intervention period. Participants’ body mass and body volume were determined using air displacement plethysmography (BodPod, CosMed, Italy), according to the manufacturer’s protocol, as reported previously. ⁷⁷

Sleep and mood questionnaires

Each morning after participants woke up, participants completed the Leeds Sleeping Evaluation Questionnaire (LSEQ). ⁷⁸ On day 2 they also filled in the Pittsburgh Sleep Quality Index (PSQI) questionnaire, which provides information on sleep quality over the previous four weeks. ⁷⁹ At the end of each office day (day 1 to 4, at 16:45h) participants also completed a mood and comfort questionnaire (e.g. visual analogue scales).

Indirect calorimetry

On the evening of day 3 (from 18:00h onwards) participants entered a respiration chamber, in which they stayed until 07:00h in the morning of day 4. During this time the oxygen consumption and carbon dioxide production were continuously measured (Omnical, Maastricht Instruments, Maastricht, The Netherlands) and further used to calculate whole-body energy expenditure, the respiratory exchange ratio (RER) and carbohydrate and fat oxidation. On day 4, oxygen consumption and carbon dioxide production were measured via a ventilated hood system while resting on a bed for 30 minutes at 08:30, 13:00, 18:00 and 22:00h (Omnical, Maastricht Instruments, Maastricht, The Netherlands). The day 4 measurements at 08:30 and 13:00h were conducted in the respective office light setting whereas measurements at 18:00 and 22:00h were conducted under dim light conditions. Energy expenditure and

substrate oxidation were calculated using the Brouwer equation⁸⁰ with protein oxidation being estimated as 12.4% of energy expenditure. Sleeping metabolic rate was defined as the lowest continuous 3-hour period of energy expenditure during the night spent in the respiration chamber.

Ambient, skin and core body temperature

Ambient temperature was continuously monitored in every room, in which participants spent time across the 4.5-day interventions. For that purpose, a mobile thermometer (ThermoPro, Canada) was positioned at desk height in the respective office light condition as well as in the bedrooms in which participants spent evenings and nights. Temperature data were logged bihourly during daytime (07:00–23:00h). From day 3 at 08:00h to day 4 at 08:00h, skin temperatures were measured at 14 ISO-defined body sites using wireless temperature sensors (iButtons, Maxim Integrated Products, USA).⁸¹ Core body temperature (CBT) was measured using an ingestible telemetric pill (e-Celsius, BodyCap, France), which participants swallowed with the lunch meal at ~14:00 on day 3 to assess CBT over ~24 hours until the pill was excreted with the stool. The nadir in CBT is often used as an indicator of circadian phase⁸² besides dim-light melatonin onset (DLMO). For this purpose, we defined the nadir in CBT as the time at which the minimum CBT occurred averaged over 15-min intervals to exclude artefacts.

Blood pressure and heart rate assessment

Blood pressure and heart rate were measured at rest every hour starting at 08:00h during the waking period of day 4, and every two hours from 00:00h onwards while sleeping in the night between day 4 to day 5. During wake hours (07:00–23:00h) participants were sitting at a desk when the automated cuff (Omron Healthcare Co., Ltd., Kyoto, Japan) was applied, while participants were lying in bed from 23:00–07:00h. Blood pressure and heart rate were measured during the waking period three times for every timepoint, and systolic, diastolic and heart rate were averaged out of these three measurements for all timepoints. During the night the measurement was performed only once to minimize disturbance of sleep.

24-hour blood and evening saliva sampling

In the morning on day 4, an intravenous cannula was placed in the participants' forearm for blood draws at 08:00, 10:00, 12:00, 13:00, 14:00, 16:00, 18:00, 20:00, 22:00, 23:00, 00:00, 02:00, 04:00, 06:00 and 08:00h the next morning. Blood samples were collected in EDTA plasma and serum separator tubes and centrifuged at 1300g for 10 min at 4°C. Room temperature, respectively. Plasma and serum were pipetted in aliquots which were frozen in liquid nitrogen and stored at -80°C for later analysis.

Saliva was captured using Salivette at 18:00, 19:00, 20:00, 20:30, 21:00, 21:30, 22:00, 22:30 and 23:00h during day 4. Participants chewed on a swab for approximately 2 min after which they put the swab back in the Salivette container. The container was centrifuged at 4°C for 2 minutes at 1000g. The saliva was pipetted in aliquots, which were frozen in liquid nitrogen and stored at -80°C for later analysis.

Skeletal muscle biopsy

On the morning of day 5 between 07:45 and 08:45h, a skeletal muscle biopsy was taken in the overnight fasted state. The muscle biopsy was taken from the muscle *vastus lateralis* under local anesthesia (1% lidocaine, without epinephrine) according to the Bergstrom technique.⁸³ The leg in which the muscle biopsy was taken during the first intervention period was randomized, and in the second intervention period the biopsy was taken from the opposite leg. Part of the muscle biopsy (50–100mg) was processed for isolation of human primary muscle satellite cells. Subsequently myogenic human primary muscle satellite cells were selected with MACS cell sorting using a mouse CD56-antibody as previously described.⁸⁴ The remaining muscle samples were freed from any visible non-muscle material, directly frozen in melting isopentane and stored at -80°C for later analysis.

Mixed meal tolerance test

In the morning of day 5, a mixed meal tolerance test (MMTT) was performed. At approximately 09:00h participants consumed a meal shake (Ensure Plus, Abbott Laboratories, USA) with the same energy content as their daily breakfast of the meal plan. Macronutrient and energy composition per 100ml of the shake were 16.8g carbohydrates, 9.1g protein, 4.8g fat and 150kcal. Blood samples were taken during the MMTT at 0, 15, 30, 45, 60, 90, 120, 150, 180 and 240 min after consumption of the meal. Indirect calorimetry was performed at 30, 60, 120, 180, and 240 min. Unfortunately, baseline indirect calorimetry measurements could not be performed due to logistical reasons. Plasma glucose, free fatty acids and serum triacylglycerol levels were determined as described above, whereas insulin levels were measured in serum with an ELISA kit (Crystal Chem, Elk Grove Village, USA).

Salivary melatonin assessment

Melatonin concentration was measured by Radio-immuno-assay (RK-DSM2 of Novolytix, Basel, Switzerland). Intra-assay CV was 32.5% for low concentrations (1.0pg/ml) and 10.9% for high concentrations (13.9pg/ml). Inter-assay CV was 30.9% for low concentrations (0.9pg/ml) and 8.7% for high concentrations (15.3pg/ml). The lower limit of quantification was 0.33pg/ml. Dim-light melatonin onset (DLMO) was determined according to St. Hilaire & Lockley.⁸⁵ In short, the DLMO threshold was set to 3pg/ml, and after first exceeding 3pg/ml, melatonin concentrations had to be higher than or equal to 3pg/ml for the next two timepoints to fulfil the DLMO criterion (if these timepoints were available). Exact DLMO was calculated by linear interpolation between the last point before and the first point that reached the DLMO criterion. If for at least one light condition, no DLMO could be detected over the saliva

sampling period ($n=3$) or if melatonin concentration were above 3 pg/ml from 18:00 onwards ($n=1$), individuals were excluded from further DLMO analyses.

Plasma, serum and monocyte analysis

Plasma glucose, free fatty acids and serum triacylglycerol were measured colorimetrically using a Cobas Pentra C400 analyser (Horiba, Montpellier, France). Serum metabolomics and lipidomics analyses, as well as monocyte transcriptomics, were carried out in samples obtained at 08:00 and 16:00 h on day 4. For metabolomics/lipidomics, twenty microliters of serum were spiked with a mixture of heavy isotopes of labelled internal standards. Samples for metabolomics were extracted using methanol and were run using a 1290 Infinity II UHPLC system (Agilent Technologies) coupled with a 6470 triple quadrupole mass spectrometer (Agilent Technologies) for the LC-MS/MS analysis. For lipidomic analysis, samples were extracted with methyl tert-butyl ether and methanol.⁸⁶ The LC-MS analysis was performed using a Vanquish UHPLC system (ThermoFisher Scientific) combined with an Orbitrap Fusion Lumos Tribrid mass spectrometer (ThermoFisher Scientific), as previously described.^{40,87,88} Missing data were imputed as 1/5th of the lowest value per metabolite and lipid. Data were scaled, probabilistic quotient normalized and log₂ transformed.

For blood monocyte isolation, 8 mL blood was collected in a CPT-tube (BD Vacutainer CPT, BD, Franklin Lakes, USA) and centrifuged for 20 min at 1800 g. Thereafter, mononuclear cells were collected and washed with PBS, centrifuged for 8 min at 350 g. Cells were frozen at -80 °C in a freezing medium containing 10% DMSO. CD14+ magnetic beads (Miltenyi Biotec) were added to thawed mononuclear cells (20 μ l per 10⁷ cells) and the mixture was incubated for 15 min at 4 °C. After incubation, the sample was washed with 2 mL of separation buffer per 10⁷ cells and centrifuged at 500 g for 10 min at room temperature without brake. The supernatant was discarded, and separation was performed using an Automacs pro-separator (Miltenyi Biotec) under the “Posselweb” program. The resulting monocyte fraction was centrifuged at 330 g for 10 min at 4 °C, resuspended in PBS, and centrifuged again at 700 g for 3 min. The final monocyte pellet was stored at -80 °C until further use.

Serum mass spectrometry analyses

For the metabolomics analysis, the chromatographic separation for samples was carried out on a ZORBAX RRH Extend-C18, 2.1 \times 150 mm, 1.8 μ m analytical column (Agilent Technologies). The column was maintained at 40 °C and 4 μ l of sample was injected per run. The mobile phase A was 3% methanol (v/v), 10 mM tributylamine, 15 mM acetic acid in water and mobile phase B was 10 mM tributylamine, 15 mM acetic acid in methanol, using a gradient with 22 min duration. The triple quadrupole mass spectrometer was operated in negative electrospray ionization mode. The metabolites of interest were detected using a dynamic MRM mode. PeakBot software (vers. 0.9.54) was used for data processing. Ten-point calibration curves with internal standardization were constructed for absolute quantification of metabolites.

For the lipidomic analysis, lipid separation was performed by reversed phase chromatography employing an Accucore C18, 2.6 μ m, 150 \times 2 mm (ThermoFisher Scientific) analytical column at a column temperature of 35 °C. A mobile phase A of acetonitrile/water (50/50, v/v) solution containing 10 mM ammonium formate and 0.1% formic acid was used. Mobile phase B consisted of acetonitrile/isopropanol/water (10/88/2, v/v/v) containing 10 mM ammonium formate and 0.1% formic acid. The flow rate was set to 400 μ l/min. The mass spectrometer was operated in ESI-positive and -negative mode and the Orbitrap MS was set in scan mode at 120,000 mass resolution within a range from 250–1200 m/z. The data analysis was performed using the TraceFinders software (ThermoFisher Scientific). Missing data were imputed as 1/5th of the lowest value per lipid. Data were scaled, mean-centered and log₂ transformed.

Monocyte transcriptomic analyses

RNA quantification was performed with a Qubit fluorimeter (ThermoFisher Scientific) and RNA integrity assessed with a Bioanalyzer (Agilent Technologies). The Illumina Stranded mRNA Prep kit (Illumina) was used for the library preparation with 200 ng of total RNA as input. Library molarity and quality were assessed with the Qubit and TapeStation (Agilent Technologies). Libraries were sequenced on a NovaSeq 6000 sequencer (Illumina) using 100-bp single-end reads protocol at the iGE3 Genomics Platform of the University of Geneva. Quality control was performed with FastQC v. 0.11.9. The reads were aligned with STAR v. 2.7.0f to the human UCSC genome hg38. The gene expression was quantified with HTSeq v. 0.9.1.⁷¹ Filtering out lowly expressed genes, normalization and differential expression analysis were performed with the R/Bioconductor package edgeR v. 3.38.4.⁸⁹ Statistical significance was assessed with a general linear model, negative binomial distribution, and quasi-likelihood F test. Over-representation analysis of Gene Ontology terms and KEGG pathways were performed with the R/Bioconductor packages: clusterProfiler v. 4.9.0 and org.Hs.eg.db v. 3.15.0. Transcript differential expression and gene set enrichment analyses were done using the limma package (version 3.58.1) in R (version 4.3.1), using the Bader Lab gene set resource (<https://www.baderlab.org/>) with clustering done using EnrichmentMap and AutoAnnotate.⁹⁰

Muscle gene transcript quantification

Part of the muscle material (10 mg) was used for RNA isolation and gene transcript abundance determination by real-time PCR as described in Harmsen et al.⁹¹ To minimize the variability in reference gene normalization, the geometric mean of two reference genes (RPL26 and RPLP0) was used as the internal reference for comparative gene expression analysis between conditions⁹² for *Bmal1*, *Clock*, *Cry1*, *Per1*, *Per2*, *Per3*, *Reverba*, and *Rora*.

Primary human skeletal myotube culture and lentiviral transduction

Primary myoblasts were cultured in Ham's F-10 Nutrient Mix, GlutaMAX Supplement medium (Gibco, Paisley, Scotland, UK), enriched in 20% fetal bovine serum (Gibco, Paisley, Scotland, UK), 1% penicillin/streptomycin (Gibco, Paisley, Scotland, UK), 0.5% gentamycin (Sigma Aldrich, Saint Louis, USA) and 1:500 amphotericin B (Gibco, Paisley, Scotland, UK) until reaching the 60–70% of confluence. Myoblasts were transduced with BMAL1-luciferase (BMAL1-luc) lentivectors at MOI=3.³⁸ After reaching 90–100% of confluence, myoblasts were differentiated into myotubes for 4–6 days in DMEM 1 g/ml glucose, pyruvate (Gibco, Paisley, Scotland, UK) supplemented in 2% fetal bovine serum (Gibco, Paisley, Scotland, UK), 1% penicillin/streptomycin (Gibco, Paisley, Scotland, UK), 0.5% gentamycin (Sigma Aldrich, Saint Louis, USA) and 1:500 amphotericin B (Gibco, Paisley, Scotland, UK).

Real-time bioluminescence recording and analysis

Differentiated myotubes were synchronized with 10 μ M forskolin (Sigma Aldrich, Saint Louis, USA) and incubated for 1 h at 37 °C. Next, the culture medium was replaced with recording medium containing 100 μ M luciferin (Nanolight Technology) and cells were placed in 37 °C Actimetrics LumiCycle, as previously described,^{37,38,87} for real-time recording of BMAL1-luc bioluminescence for the duration of 96 h. Generated bioluminescence profiles were normalized to the moving average of 24 h (detrended).⁹³ Circadian parameters were calculated based on detrended data using the Chronostar 3.0 software⁹⁴ with the sinusoid function fit to the 12–100 h data range. We used Partial Least Squares Regression (PLSR) to predict the bioluminescence phase using clock gene expression. We used the function 'PLS Regression' within scikit-learn (v1.0.2) and with `n_components=1`. We used all data from both conditions, and we used a leave-participant-out cross-validation prediction approach to avoid the same participant being in the training and test set. The model was trained on all data excluding one participant, and then the model was used to predict the test participant values. This procedure was performed for all participants. The model was then trained on all participants to retrieve the model parameters.

QUANTIFICATION AND STATISTICAL ANALYSIS

A 2-way repeated measures ANOVA with time and condition (condition: natural vs. artificial office light) and their interaction as fixed effects was applied to test for differences over time between natural and artificial office light in 24-hour plasma metabolites, substrate metabolism and energy expenditure, core and skin temperature, blood pressure and heart rate. In case of individual missing time points, a generalized linear mixed model was run instead of the 2-way repeated measures ANOVA. In the absence of interaction, we interpreted the main effect for condition, and in the case of statistical significance, we followed up the condition effect with pairwise comparisons per time point using Bonferroni post-hoc tests. Paired t-tests were conducted to detect differences between natural vs. artificial office light in all other outcomes without repeated measures, and Wilcoxon tests were performed for non-normally distributed data. If completed data was not available for certain outcomes for all participants ($n=13$), mostly due to technical issues during individual measurements, the respective applicable sample size is stated in the respective figure legends.

Differences in serum metabolites, lipid families, lipid species, and blood monocyte transcripts between natural and artificial light conditions were modelled using Orthogonal Partial Least Squares Discriminant Analysis (OPLS-DA).⁹⁵ Separate OPLS-DA models were built for each dataset at the 08:00 and 16:00 h time points using `ropls`. From the predictive component of each OPLS-DA model, correlation-scaled loadings ($p(\text{corr})$) were obtained for each feature. Statistically, the correlation-scaled loading ($p(\text{corr})$) for a given molecule quantifies the Pearson correlation between that molecule's abundance profile across the samples and the model's predictive score (component) that maximally separates the groups. To compare targets across time points, Shared and Unique Structures (SUS) plots were constructed.⁹⁶ For each target, the $p(\text{corr})$ value from the 16:00 h model (X-axis) was plotted against the $p(\text{corr})$ value from the 08:00 h model (Y-axis).

For machine learning analyses of the omics datasets, the `caret` package (version 6.0.94) in R was utilized, incorporating a leave-one-participant-out cross-validation approach. This ensured that all data points from an individual participant were excluded from the training set when evaluating the same participant in the test set. To enhance classification performance of light and time conditions, recursive feature elimination was applied to identify the most predictive variables. To ensure the reproducibility of the classification accuracy of the machine learning models, each omics dataset (metabolomic, lipidomic and transcriptomic) was partitioned into training and test sets and run using 200 unique seeds. Data are represented as mean \pm SEM (standard error of the mean) unless indicated otherwise. The level of significance was set to <0.05 for all analyses.